Since January 2020 Elsevier has created a COVID-19 resource centre with free information in English and Mandarin on the novel coronavirus COVID-19. The COVID-19 resource centre is hosted on Elsevier Connect, the company's public news and information website.

Trends in Analytical Chemistry 85 (2016) 36–60

Contents lists available at ScienceDirect

Trends in Analytical Chemistry

journal homepage: www.elsevier.com/locate/trac

Critical overview on the application of sensors and biosensors for clinical analysis

Celine I.L. Justino [a,b,*], Armando C. Duarte [a], Teresa A.P. Rocha-Santos [a]

[a] Department of Chemistry & CESAM, University of Aveiro, Campus de Santiago, 3810-193 Aveiro, Portugal
[b] ISEIT/Viseu, Instituto Piaget, Estrada do Alto do Gaio, Galifonge, 3515-776 Lordosa, Viseu, Portugal

ARTICLE INFO

Keywords:
Analytical performance
Biosensor
Clinical analysis
Figure of merit
Sensor

ABSTRACT

Sensors and biosensors have been increasingly used for clinical analysis due to their miniaturization and portability, allowing the construction of diagnostic devices for point-of-care testing. This paper presents an up-to-date overview and comparison of the analytical performance of sensors and biosensors recently used in clinical analysis. This includes cancer and cardiac biomarkers, hormones, biomolecules, neurotransmitters, bacteria, virus and cancer cells, along with related significant advances since 2011. Some methods of enhancing the analytical performance of sensors and biosensors through their figures of merit are also discussed.

Contents

* Corresponding author. Tel.: +351 232 910 100; Fax: +351 232 910 183.
E-mail address: celinejustino@ua.pt (C.I.L. Justino).

http://dx.doi.org/10.1016/j.trac.2016.04.004
0165-9936/

1. Introduction

Technologies for improving global health services are in great demand, in the diagnosis, treatment and prevention of diseases [1]. Although effective, the laboratory techniques based primarily on the optical analytical principle, such as immunoassays, require sample enrichment and purification before analysis. Moreover, they are expensive and slow. Thus, strategies for signal amplification have been recently proposed to increase immunoassay sensitivity for further clinical diagnostics [2]. Sensors and biosensors have been extensively studied for their role in detecting and monitoring different types of analytes for food safety, environmental monitoring, clinical analysis and medical diagnosis [3]. Immunosensors have been considered in clinical diagnostics for the detection and identification of cardiac and cancer biomarkers. This is key to developing point-of-care technologies that can analyse real biological samples (for continuous monitoring of physiologically important analytes) in routine clinical use [4].

Three main types of sensors and biosensors are commonly used based on their transduction principle: electrochemical, optical and piezoelectric-based sensors and biosensors. Electrochemical biosensors are self-contained integrated devices that can provide specific quantitative or semiquantitative analytical information using a biological recognition element in direct contact with an electrochemical transduction element (e.g., a pair of electrodes or field-effect transistors (FETs)) [5]. Thus, electrochemical biosensors monitor electroactive species that are produced or consumed by the action of the biological elements, based on potentiometric, amperometric or impedimetric transduction principles [6]. The analytical output in optical sensors is a result of the interaction of the analyte with the transducer in terms of optical properties such as absorbance, reflectance, luminescence, fluorescence, refractive index and surface plasmon resonance (SPR) [6]. Piezoelectric sensors employ materials that resonate when an external alternating electrical field is applied. Here, quartz crystals are used to produce an oscillating electric field in which the resonant frequency of the crystal depends on its chemical nature, size, shape and mass [6]. According to recent studies, the electrochemical principle is mainly applied in clinical sensors and biosensors [4,7–10]. For example, electrochemical immunosensors are used in clinical diagnostics as point-of-care devices, as they are portable, simple, easy to use, cost-effective and disposable in most cases. Furthermore, studies have demonstrated the benefits of using electrochemical immunosensors for cardiac and cancer biomarkers [4]. In addition, various nanomaterials can be incorporated into electrochemical biosensors for additional benefits [1]. Similarly, implantable electrochemical biosensors can be used as point-of-care devices to monitor individual subjects continuously *in vivo* and make a personalized diagnosis, as several functions are combined in individual microchips [1,11].

Sensors are also classified by the recognition principle of the analyte of interest: immunosensors (antibody–antigen interaction) and enzymatic biosensors (enzyme–target analyte interaction). Both classical (enzymes and antibodies) and recent recognition elements play a key role in chemical sensors and biosensors by recognizing the target analytes of interest [12].

In recent years, nanomaterials have been incorporated into clinical sensors and biosensors for their conductive properties, high surface-to-volume ratio and good biocompatibility, thus enhancing performance [13–15]. For example, to detect clinically significant biomarkers, the following nanomaterials have been incorporated into sensors: nanowires (NWs) synthesized from metals (e.g., Ni, Cu, Au and Pt), metal oxides (ZnO, SnO_2 and Fe_2O_3) and silicon/indium/gallium semiconductors (Si, InP, GaN); quantum dots based on CdSe, CdTe or CdSeTe; carbon nanotubes (CNTs); and metal nanoparticles (based on Au, Cu, Pd, Co, Ag or Pt) [1,9,13]. CNTs have been used as transduction elements in biosensors to detect and quantify proteins, neurotransmitters and cancer biomarkers [1]. In addition, nanotechnologies help miniaturize biosensing platforms, thus consuming lesser power, and requiring lower sample volumes, shorter assay times and low operating costs. Furthermore, when used in sensors and biosensors, NWs confer several nanomaterial properties such as mechanical stiffness, high carrier mobility, thermal conductivity, high surface-to-volume ratio and improved electron transfer of CNT, as well as the high surface-to-volume ratio and electrical current capacity [13].

The analytical performance ultimately determines the final prototypes of clinical sensors and biosensors for commercial use, primarily for glucose biosensors [16]. Several methods have been proposed to enhance the analytical performance of sensors by improving the figures of merit, particularly for more sensitive and reproducible sensing platforms. For example, nanomaterials have been found to improve the sensitivity and the stability of the analytical response of sensors and biosensors either in the transduction substrate or in association with metal nanoparticles or polymers.

As sensors and biosensors are essential for clinical analysis, we present an update on a previous literature review published in 2010 by Justino et al. [3]. Thus, the present paper aims to review the state of the art of recent sensors and biosensors used for clinical analysis covering the period 2011–2015. Their analytical performance is compared, and their advantages and limitations described based on the transduction principle. Some approaches to improve the analytical performance of sensors and biosensors are also reported.

2. Analytical figures of merit

A method is validated by assessing its figures of merit. These are quantifiable terms that may indicate the quality of the process, which in turn ensure the quality of results [17]. Similarly, the main figures of merit to be considered for validating sensors and biosensors are sensitivity, selectivity, limit of detection (LOD), repeatability and reproducibility [3]. Such figures of merit should also be characterized so as to compare the analytical performance of sensors and biosensors. Table 1 shows the definitions of the main figures of merit used to validate an analytical method such as sensors and biosensors.

The figures of merit should be assessed during the development stage and be verified periodically during routine use, to estimate analytical performance characteristics such as reliability, capacity and variability.

Table 1
Main figures of merit used to validate sensors and biosensors [3,17]

Figure of merit	Definition
Sensitivity	Slope of the analytical calibration curve. An analytical method is sensitive when a small change in analyte concentration causes a large change in response.
Selectivity	Ratio of the slopes of the calibration lines of the analyte of interest and a particular interference. A method is selective when the response of the analyte can be differentiated from every other response.
LOD	Concentration or the quantity derived from the smallest signal that can be detected with acceptable degree of certainty for a given analytical procedure.
Repeatability	Closeness of the agreement between successive measurements of the same parameter, which were carried out in the same conditions related to operators, apparatus, laboratories and/or intervals of time analysis.
Reproducibility	Closeness of the agreement between successive measurements of the same parameter, performed in different conditions in terms of operators, apparatus, laboratories and/or intervals of time analysis.
Signal-to-noise ratio	Ratio of the useful analytical signal to the background noise, which is identified as a measure of the statistical fluctuations in a blank signal.

3. Improvement of the analytical performance of sensors and biosensors

Improving the analytical performance of sensors and biosensors is essential for producing prototypes and in turn commercializing these systems, for example, in environmental monitoring, food safety or clinical analysis. Thus, recent research has focused on enhancing the analytical performance of sensors and biosensors by enhancing the associated figures of merit. Sensitivity is a key figure of merit. Based on classical (univariate) calibration, it is defined by the change in analytical response of the instrument divided by the corresponding change in stimulus (concentration of the analyte of interest), that is the slope of the analytical calibration curve [17]. Nanotechnology has been applied to enhance the performance of biosensors. Nanostructures offer a large surface area-to-volume ratio to immobilize labels and biological recognition elements, thus amplifying the analytical signal and improving sensitivity [18].

3.1. Types and characteristics of nanomaterials

Nanomaterials have been incorporated into sensors and biosensors to increase biocompatibility, additional binding sites and signal intensities (through enhanced electrical properties), thus improving the sensitivity and specificity of the detection [14,19]. In their work, Zhang et al. [20], Zhang et al. [21], Baek et al. [22], Feng et al. [23], Wang et al. [24], Wang and Zheng [25], Lozano et al. [26], Guo et al. [27] and Sun et al. [28] studied the effect of nanomaterials (i.e., gold nanoparticles, ZnO nanoparticles, ZnO–gold nanocomposites and CNTs) on the analytical performance of sensors and biosensors (i.e., in terms of sensitivity, LOD, concentration range and stability). In their study on electrochemical DNA sensors, Zhang et al. [20] showed that the presence of gold nanoparticles significantly enhanced the sensitivity and LOD. In the absence of gold nanoparticles, the peak current was found to increase only slightly upon hybridization with 1 μM DNA target. Upon amplification with gold nanoparticles, the peak current was significantly enhanced even with a 10-pM DNA target. Thus, the presence of gold nanoparticles allows highly sensitive DNA detection [20]. Moreover, the LOD (10 fM) is lower with gold amplification, as the sensor only detects a 0.5-nM target DNA without gold nanoparticle amplification. Zhang et al. [21] also showed an improvement in LOD with the incorporation of gold nanoparticles. They [21] developed a microfluidic bead-based immunosensor to detect α-fetoprotein using horseradish peroxidase coupled with gold nanoparticles for signal amplification. The sensitivity of the target analyte was significantly enhanced, as the gold nanoparticles offered a large surface area for the binding of enzymes on each nanosphere [21]. The immunosensor showed a 50-fold increase in LOD compared with immunosensors without gold nanoparticles. Baek et al. [22] developed an optical sensor for thrombin based on the SPR principle. They applied a dual-nanoparticle amplification strategy: gold nanoparticles of two different shapes (nanorods and quasi-spherical nanoparticles) were incorporated in the sensor. With real-time SPR measurements to detect target concentrations as low as 0.1 aM, the authors found a 10-fold improvement compared to methods that used only single nanoparticles [22]. Feng et al. [23] showed that the LOD of electrochemical sensors used in DNA hybridization recognition was significantly enhanced. This was a result of the synergistic effect of two nanomaterials (gold nanoparticles and polyaniline nanotube membranes), a combination of very large surface areas and excellent conductivities. These sensors display a significantly lower LOD (3.1×10^{-13} mol L^{-1}) for DNA detection versus the LOD ranging from 1.4×10^{-12} to 2.4×10^{-11} mol L^{-1} for other sensors [23]. Incorporating metal semiconductor compounds such as ZnO in conjugation with gold nanoparticles can enhance the detection sensitivity of SPR sensors. In this respect, Wang et al. [24] developed an SPR biosensor based on ZnO–gold nanocomposites to detect human immunoglobulin M (hIgM). The biosensor displays an analytical response to hIgM in the concentration range of 0.30–20.00 μg mL^{-1}. Without ZnO–gold nanocomposites, the biosensor responds to hIgM in the concentration range of 1.25–20.00 μg mL^{-1}. Wang et al. [24] also showed enhanced sensitivity of biosensors based on ZnO–gold nanocomposites to determine hIgM. They reported a maximum shift of resonant wavelength (analytical response at 20.00 μg mL^{-1}) of 7.53 nm compared to the 4.10 nm in sensors with a gold film only. In another work, Wang and Zheng [25] reported the threefold improved sensitivity of an electrochemical sensor based on glass carbon electrode for hydrogen peroxide with the electrodeposition of silver nanoparticles on a ZnO film, compared with similar sensors without ZnO. The improved stability of sensors with ZnO was verified by a 2% decrease in analytical response, compared with the 30% drop in response for sensors without ZnO films. According to Wang and Zheng [25], ZnO immobilizes inorganic nanoparticles, facilitates the formation and more intensive distribution of small silver nanoparticles and thus improves the stability of the sensor. Lozano et al. [26] developed an electrochemical sensor based on a CNT paste electrode (CNTPE) with polymer electrogenerated from Fe(III)-5-amino-1,10-phenanthroline solution for detecting glucose, compared with a similar sensor based on graphite paste electrode (CPE). The CNT was found to be crucial for generating poly(Fe(III)-5-amino-1,10-phenanthroline). In turn, the CNTPE/poly(Fe(III)-5-amino-1,10-phenanthroline) increased the sensitivity 200-fold at –0.100 V (sensitivity of 130 μA M^{-1}), versus that obtained with CPE/poly(Fe(III)-5-amino-1,10-phenanthroline) with a sensitivity of 0.65 μA M^{-1}. Guo et al. [27] recently studied the effect of gold nanoparticle aggregation in DNA colorimetric sensors. Gold dimers (selectively formed upon target binding) significantly improved the long-term stability (approximately 10-fold) and the dynamic range of detection (approximately more than two orders of magnitude) compared with conventional colorimetric sensors, which had larger nanoparticle aggregates. Sun et al. [28] proposed a multilayer film based on gold nanoparticles and polyaniline/carboxylated multiwalled CNT (MWCNT)–chitosan nanocomposites used in an electrochemical immunosensor to detect chlorpyrifos. The analytical response of the immunosensor – in terms of the change in reduction peak current before and after immunoreaction – was enhanced after the gold nanoparticles were adsorbed onto the surface of the polyaniline/carboxylated MWCNT–chitosan nanocomposite film due to fast direct electron transfer, facilitated by the gold nanoparticles [28]. Thus, the authors concluded that gold nanoparticles on the nanocomposite film enhance the electrochemical signal and adsorption capacity of antibodies, ultimately enhancing the detection sensitivity. Wei et al. [29] studied electrochemical sensors using multilayer electrodes, that is, thin layers of polymers, nanoparticles or nanoparticle–polymer composites stacked on top of the electrode. They attributed the high sensitivity of these sensors to their action as a three-dimensional (3D) matrix for capturing nucleotide probes and reducing interference from nonspecific molecules, which can contribute to background noise.

Other researchers have reported enhanced analytical signal and sensitivity with the incorporation of gold nanoparticles, quantum dots and graphene [30–33]. For example, Kavosi et al. [30] constructed an electrochemical immunosensor to detect α-fetoprotein. In this sensor, polyamidoamine dendrimer-encapsulated gold nanoparticles were immobilized as the sensing interface on a gold electrode. The gold nanocomposite increased the sensitivity of the immunosensor, as it amplified the signal due to its high conductivity and remarkably large surface area [30]. According to the authors, only a small response was noted when α-fetoprotein was incubated with its antibody being directly exposed to the gold electrode, as well as a slightly larger response (10-fold increase) when α-fetoprotein interacted with the gold nanocomposite-modified

electrode. The signal amplification was attributed to the large specific surface area of the gold nanocomposite, which possessed several surface functional groups that captured more antibodies at the sensing interface, and the accelerated electron transfer [30]. Quantum dots, nanoparticles with ten thousands of metal ions, can also be used for signal amplification of sensors. For example, Zhou et al. [31] incorporated CdS quantum dots and gold nanoparticles labelled with antibodies into an electrochemiluminescence immunosensor to detect α-fetoprotein with amplified signal. According to the authors, the signal intensity from the CdS/gold composite film is about 2.5-fold higher than that from the pure CdS film. This was attributed to the significant catalytic activity and enhanced electrical conductivity of the gold nanoparticles, which in turn increased the detection sensitivity [31]. Xie et al. [32] fabricated an electrogenerated chemiluminescence assay to detect thrombin, using CdSe/ZnS quantum dots as sensing probe on a graphene-modified glassy carbon electrode covered with gold nanoparticles. Xie et al. [32] confirmed that the analytical signal in the absence of quantum dots was very low; further, the electrogenerated chemiluminescence intensity increased greatly with the addition of quantum dots (coupled with avidin and DNA). Du et al. [33] incorporated graphene sheets in the sensor platform and functionalized carbon nanospheres labelled with horseradish peroxidase in an electrochemical immunosensor to detect α-fetoprotein with dual signal amplification. Thus, the graphene-modified immunosensor with carbon nanosphere labelling showed a sevenfold increase in detection signal and enhanced sensitivity compared to conventional unmodified immunosensors [33]. According to the authors, graphene offers a large surface area to capture more antibodies on the electrode surface, in addition to accelerating electron transfer, thus amplifying the signal.

3.1.1. Density of nanomaterials and width of nanomaterial channels

Nanomaterials characteristics such as CNT density [34–36] and CNT width channel [37] have been shown to affect the analytical performance of sensors and biosensors, due to their effect on figures of merit such as the signal-to-noise ratio, reproducibility, sensitivity and LOD. Ishikawa et al. [35] studied the effect of controlling the density of a network of single-walled CNTs (SWCNTs) on the analytical performance of FET devices. They classified the density of nanotubes as low, medium and high based on the time of incubation in ferritin solution, which is associated with the density of the catalyst. Ishikawa et al. [35] concluded that the lower the CNT density the higher the sensitivity in relation to LOD and magnitude of response, as well as the reproducibility of such biosensors. They [35] attributed the increased sensitivity arising from the low density of SWCNTs in part to the elimination of direct metallic nanotube pathways. This enhances the semiconductor behaviour of nanotubes, lowers the capacitance and increases the ON/OFF ratios, whereas the high density of SWCNTs reflects their quasi-metallic behaviour. The sensing performance of these devices was investigated using streptavidin as a model analyte. However, the optimized FET devices were ultimately used to detect nucleocaspid protein, a biomarker associated with severe acute respiratory syndrome (SARS) coronavirus. Based on the plot of the analytical signal (normalized conductance *vs.* log of the streptavidin concentration) of each device with different nanotube density, devices with low density of nanotubes showed the strongest response whereas those with a high density of nanotubes showed the weakest response. The LOD was estimated to range from 100 pM to 1 nM, 10 to 100 pM and 1 pM to 10 pM for high-, medium- and low-density devices, respectively. Fu et al. [34] also verified the effect of nanotube density on the sensitivity of FET devices. In FET biosensors with networks of SWCNTs for detecting DNA molecules, they found that the nanotube density increased the ON/OFF ratios from 5 to 2000 with high and low SWCNT density, respectively, and increased the LOD from 10 pM to 0.1 fM with high and low SWCNT density, respectively. The DNA molecules served as impurities and caused carrier charge scattering, which significantly increased the ON/OFF ratio. The ON/OFF ratio increased more with lower SWCNT densities, due to lesser number of metallic SWCNT percolative paths. Recently, Okuda et al. [36] designed a electrolyte-gated sensor based on an FET composed of horizontally aligned multiple SWCNTs synthesized on single-crystal quartz for the label-free immunosensing of human immunoglobulin E. The drain current (analytical response) of the sensors with aligned channels exhibited a drain current 400 times that of single-channel devices, with considerably smaller fluctuations in drain current. The calculated residual standard deviation (RSD) was 2.4% and 0.05% for the single- and aligned-channel FET, respectively, which indicated their high sensitivity and easy application [36]. In studying the effect of CNT width channel on the analytical performance of sensors, Lee et al. [37] developed highly sensitive nanoscale sensors for Hg^{2+} by controlling the structure of aligned SWCNT networks. They [37] concluded that a better signal-to-noise ratio and a higher sensitivity are obtained with narrower channels than with wider channels, due to a decrease in the effective length of the current paths (i.e., damaged current paths decrease the conductivity of SWCNT channels). Moreover, the LOD increased from 10 nM using 2-μm-wide SWCNT network sensors to 1 pM using 100-nm-wide SWCNT network sensors. Lee et al. [37] also obtained mathematical relations between SWCNT channel width and sensitivity (sensitivity ~ $width^{-1.6}$) and between SWCNT channel width and signal-to-noise ratio (signal-to-noise ratio ~ $width^{-1.1}$).

3.1.2. Number, diameter and doping level of nanomaterials

Other nanomaterial characteristics such as number, diameter and doping level of nanomaterials also affect the figures of merit of sensors. The sensitivity of sensors can be enhanced by using low NWs, larger NW diameters and lower doping concentration and by improving the LOD in sensors with lower doping concentration. In their work, Li et al. [38] tested sensors based on NWs to detect human immunoglobulin G (hIgG) as a model analyte. On testing NW-based sensors with different numbers of NWs, Li et al. [38] revealed a decrease in sensitivity with increasing number of NWs; that is, devices with a larger number of NWs (four and seven NW-based devices) were less sensitive (decrease of ~38 and ~82%, respectively) than those with just one NW. The authors attribute this decrease in sensitivity to the depletion of hIgG molecules from the surrounding solution. This reduces the binding events between the NW and analyte, resulting in smaller current changes in these sensing devices. Li et al. [38] tested NW-based sensors with different NW diameters ranging from 60 to 80, 81 to 100 and 101 to 120 nm. They found that sensors with larger NW diameter (81–100 and 101–120 nm) exhibited a greater decrease in sensitivity (~37%) compared to devices with thinner NWs of 60–80-nm diameter (decrease in sensitivity of ~16%). This was due to the decrease in the surface-to-volume ratio of thick wires at the micrometre order. Conversely, Li et al. [38] noted that a change in doping concentration by two orders of magnitude increased the biosensor sensitivity 3.2-fold; that is, a 69% increase in sensitivity led to a decrease in NW doping from 10^{19} to 10^{17} atoms cm^{-3}. Li et al. [38] also observed that NW-based sensors with a doping concentration of 10^{17} atoms cm^{-3} had a lower LOD for hIgG (~10 fg mL^{-1}) than sensors with 10^{19} (LOD of ~10 pg mL^{-1}).

3.2. Presence of labelled molecules

In immunoassays and other analytical techniques, as well as sensors and biosensors, labels aid in the rapid detection of the target analyte, by amplifying the analytical signal. For example, fluorescence-based labelling methods were found to be more sensitive and specific than label-free methods [39]. Recently, Granqvist et al. [39] proposed an optical biosensor based on the SPR principle,

with the presence of labelled molecules (strongly absorbing dye molecules) significantly enhancing the sensitivity and specificity of the SPR sensor. Two simple model assays were used to demonstrate the performance of this method: the small molecule assay was used to demonstrate the increased sensitivity of label SPR, with the sensor containing bovine serum albumin (BSA) and avidin. The DNA assay was used to demonstrate the increased selectivity of the assay, with the sensor containing single-stranded DNA bound to the surface-bound avidin [39]. According to the authors, the sensitivity is significantly enhanced (100-fold) compared with conventional label-free SPR. In addition, the influence of noise factors such as temperature, pressure and bulk liquid composition variations is also significantly reduced with label-enhanced SPR sensing [39]. However, the specificity was very high and stable in the presence of the label, which reduces nonspecific binding [39].

Nanoparticles have also been used as labels in sensors and biosensors to amplify the analytical signal and increase sensitivity to target analytes. For example, Shen et al. [40] developed an electrochemiluminescence immunosensor to detect human cardiac troponin I (cTnI). They used N-(aminobutyl)-N-(ethylisoluminol)-functionalized gold nanoparticles (ABEI-functionalized gold nanoparticles) as labels for the attachment of antibodies. Here, ABEI, a derivative of isoluminol, was used as an electrochemiluminescence reagent, which is more efficient than luminol when chemically attached to specific analytes. Thus, it is a suitable label for bioassays [40]. Shen et al. [40] tested three kinds of probes including ABEI, luminol- and ABEI-functionalized gold nanoparticles. They showed that the immunoassay system using ABEI-functionalized gold nanoparticles as the label exhibited a higher analytical signal than those using other labels; that is, the electrochemiluminescence intensity of ABEI-functionalized gold nanoparticles is 12.5-fold greater than the intensity of ABEI and 1.5-fold greater than that of luminol-functionalized gold nanoparticles. Thus, the assay with ABEI-functionalized gold nanoparticles as the label showed increased sensitivity [40]. In another work, Su et al. [41] developed an electrochemical immunosensor to detect α-fetoprotein using nanogold-enclosed titania nanoparticles to label antibodies. They [41] demonstrated that the electrochemical signal was significantly amplified with nanogold-enclosed titania nanoparticles compared with pure nanogold or titania-based labels. This is in turn increased the sensitivity of the immunosensor to α-fetoprotein. Zhang et al. [42] produced an electrochemiluminescence immunosensor to detect cancer biomarkers with Ru–silica capped onto a nanoporous gold composite as the label. This electrochemiluminescence label was found to amplify the signal, greatly increase the sensitivity and extend the detectable concentration range by two orders of magnitude.

Magnetic nanoparticles can also be used as labels to enhance the sensitivity and stability of sensors and biosensors [43]. For example, Wang et al. [44] developed an SPR biosensor with magnetic nanoparticles (with iron oxide core) as labels to detect human chorionic gonadotropin. The sensitivity of the biosensor was investigated as a function of the mass transport of the analyte to the sensor surface driven by diffusion (free analyte) or by the magnetic field gradient (analyte bound to magnetic nanoparticles) [44]. According to the authors, the response of the SPR biosensor with the magnetic nanoparticles is ~17 times greater than that without magnetic nanoparticles, due to the larger mass and higher refractive index of the magnetic nanoparticles [44]. In addition, the sensitivity of human chorionic gonadotropin detection was increased by four orders of magnitude compared with the regular SPR sensor for direct detection. This was also attributed to the larger mass and higher refractive index of magnetic nanoparticles [44]. In another work, Liu et al. [45] constructed an electrochemiluminescence immunosensor to detect cancer biomarkers using CdTe quantum dot-coated silica nanospheres as labels for signal amplification. This immunosensor displayed a stronger electrochemiluminescence signal 4.1-fold that of immunosensors with pure CdTe quantum dots. Thus, this immunosensor shows increased sensitivity [45].

3.3. Nature of recognition element

Recognition elements are essential components of sensors and biosensors, as they recognize the target analytes of interest. Novel recognition elements such as aptamers, molecularly imprinted polymers, DNAzymes and affibodies have been studied for increasing detection sensitivity [12].

Aptamers have been recently used as recognition elements due to several advantages. These include thermal stability, reusability and ease of modification for their immobilization by incorporating reporter molecules (e.g., fluorophores or enzymes) and functional groups [12]. Furthermore, they offer more advantages than antibodies as they are versatile, do not need animal sources and have a higher surface density of receptors [12]. They improve the analytical performance of sensors and biosensors primarily by increasing the LOD. Yao et al. [46] compared the performance of a quartz crystal microbalance (QCM) biosensor using two types of recognition elements, aptamer and antibody, in detecting immunoglobulin E (IgE) in human serum. Aptamers or antibodies specific to IgE were immobilized on the gold surface of a quartz crystal, and the frequency shifts of the QCM were measured. The linear range of the antibody-based QCM (10–240 $\mu g\ L^{-1}$) was comparable to that of the aptamer-based QCM (2.5–200 $\mu g\ L^{-1}$); however, a lower LOD was reported in the latter (2.5 $\mu g\ L^{-1}$) than in the former (10 $\mu g\ L^{-1}$). The authors contended that the aptamers could tolerate the repeated affine layer regeneration after ligand binding, recycling the biosensor with little loss of sensitivity. When stored for three weeks, the frequency shifts of the aptamer-coated crystals were greater than 90% of the shifts in response on the first day [46].

Enzymes and DNAzymes have also been used to enhance sensor performance in terms of sensitivity and LOD. According to Du et al. [47], enzyme-functionalized nanoparticles are widely used as labels to enhance detection sensitivity, wherein a large amount of enzyme is loaded for an individual sandwich immunological reaction event. Du et al. [47] developed an electrochemical immunosensor to detect phosphorylated p53 using graphene oxide as a nanocarrier of enzymes (horseradish peroxidase). They used a multienzyme labelling strategy instead of a single-enzyme label during the immunoassay to enhance detection sensitivity [47]. In addition, the LOD is 10-fold lesser than that of a conventional sensor with a single horseradish peroxidase label. DNAzymes, catalytic nucleic acids containing deoxyribozyme, have also been used as recognition elements. It is synthesized by the SELEX (systemic evolution of ligands by exponential enrichment) technique, generating well-ordered, three-dimensional structures that catalyse specific chemical reactions [48]. Huang et al. [49] developed a label-free colorimetric aptasensor based on DNAzyme amplification to detect thrombin. The sensor can detect thrombin specifically with an LOD of 1.5 pM, which is at least four orders of magnitude lesser than the unamplified colorimetric assay [49]. Zhao et al. [50] developed a versatile DNAzyme-based amplified biosensing platform to detect nucleic acids, proteins and enzyme activity. The fluorescence intensity and the multiple turnover capability of the activated DNAzyme were enhanced, in turn increasing the sensitivity of the sensing system [50].

Molecularly imprinted polymers have also been recently used as recognition elements. They offer several advantages such as high selectivity, stability, short time of synthesis, high thermostability and cost-effectiveness. As they can potentially replace biological antibodies, they are also known as artificial antibodies or plastic antibodies [12]. They have been used in sensors and biosensors to enhance the analytical signal, sensitivity and LOD. Gholivand et al. [51] fabricated a selective and sensitive electrochemical sensor to detect propylparaben, based on a nanosized molecularly imprinted

polymer–carbon paste electrode. This electrode possesses high recognition ability compared with a non-imprinted polymer–carbon paste electrode. The analytical signal obtained with cyclic voltammograms was recorded. The signal of the molecularly imprinted polymer-based sensor was found to be higher than that of the non-imprinted polymer-based sensor. This indicates that the molecularly imprinted polymer significantly absorbs propylparaben from the aqueous solution, compared with the non-imprinted polymer-based sensor [51]. In another work, Kong et al. [52] fabricated an electrochemical sensor for ascorbic acid using a molecularly imprinted copolymer, poly(*o*-phenylenediamine-*co*-*o*-aminophenol) as the recognition element, noting a high sensitivity and selectivity. Compared with a polypyrrole-based sensor for ascorbic acid (concentrations ranging from 250 to 7000 μM and LOD of 74 μM), the analytical performance of the imprinted copolymer sensor was enhanced (concentrations ranging between 100 and 10,000 μM, and an LOD of 50 μM). This is attributed to the broadened usable pH range of poly(*o*-phenylenediamine-*co*-*o*-aminophenol) (from pH 1.0 to pH 8.0) [52]. The sensor also showed good reproducibility and stability, and it has been successfully used to determine ascorbic acid in real samples. However, the lack of simple and robust techniques for synthesizing molecularly imprinted polymers can limit their practical applications in future. This is because different combinations between monomers and cross-linkers are needed to obtain selective molecularly imprinted polymers. The main limitation to their use in sensors and biosensors is that they cannot be easily integrated into transducers. Thus, more research into enhancing the analytical signal is needed. Protein detection is also limited with these sensors because a three-dimensional element is commonly lacking at the polymer surface.

3.4. Modes of delivering power

The modes of delivering electric power to sensors and biosensors, that is, delivering alternating current (AC) or direct current (DC) [53] and the use of a specific frequency [54], can also be considered when improving the sensor output (i.e., analytical signal). Thus, the figures of merit of these sensing systems, such as sensitivity and LOD, can be enhanced. For example, Yamamoto et al. [53] fabricated CNT-based FET biosensors to detect BSA, which showed enhanced sensitivity (by increasing the signal-to-noise ratio) with AC measurement instead of DC measurement. They showed that AC measurement with a lock-in amplifier suppresses the drain current fluctuations in these biosensors without decreasing the signal level. Thus, the noise level of FET biosensors used in buffer solutions decreased considerably with AC measurement. The signal-to-noise ratio of sensors measured using AC was six times greater than that obtained using DC. Although the sensors were tested for BSA, they can be used to detect several other compounds with the AC measurement. Recently, March et al. [54] proposed a highly sensitive and versatile QCM immunosensor with high fundamental frequency (HFF) for pesticide (carbaryl and thiabendazole) analysis. They also estimated the sensitivity of conventional QCM sensors via a novel electronic characterization approach based on phase change measurements at a constant fixed frequency. In general, the current already established, commercialized systems employ frequencies ranging from 5 to 20 MHz. However, a suitable HFF is necessary for liquid applications requiring sensitive detection of small changes [54]. March et al. [54] verified that the QCM immunosensor with an HFF of 100 MHz was most sensitive. On comparing these results with those reported for the 9-MHz QCM, an increase of one order of magnitude in sensitivity and two orders of magnitude in LOD was found (sensitivity of 30 μg L^{-1} and 0.66 μg L^{-1}, and LOD of 11 μg L^{-1} and 0.14 μg L^{-1}, for 9 and 100 MHz, respectively). A 50-MHz QCM was also tested, and both the sensitivity (1.95 μg L^{-1}) and LOD (0.23 μg L^{-1}) were found to have intermediate values in relation to the previous two tested QCM sensors [54].

4. Analytical performance of sensors and biosensors for clinical analysis

In the following subsections, the study of the analytical performance of sensors and biosensors by assessing the associated figures of merit is reported. The configuration of the various sensors and biosensors used to detect physiologically important analytes is also considered in clinical analysis.

4.1. Sensors and biosensors for cancer and cardiac biomarkers

Several publications report that sensors and biosensors are more often developed for detecting cancer and cardiac biomarkers than other groups of analytes in clinical diagnostics. This is because these biomarkers are clinically relevant and must be detected early using point-of-care diagnostic devices.

Table 2 includes the figures of merit of current sensors and biosensors (from studies published between 2011 and 2015) to compare their analytical performance in detecting 1) cancer biomarkers (e.g., prostate-specific antigen (PSA), interleukins (IL-6 and IL-8), matrix metalloproteinases (MMP-2 and MMP-3), α-fetoprotein and carcinoembryonic antigen (CEA)) and 2) cardiac biomarkers (e.g., C-reactive protein (CRP), amino-terminal pro-brain natriuretic peptide (NT-proBNP), cardiac troponins (cTnT and cTnI) and myoglobin). Table 3 lists the normal values of these physiologically important analytes.

4.1.1. Cancer biomarkers

Determining the levels of cancer biomarkers in blood or tissue is crucial for the screening of cancer. Further, developing sensitive and reliable point-of-care devices has posed a significant challenge in the early detection and monitoring of cancer, as the prerequisites are high sensitivity, accuracy, minimal technical expertise and rapid and facile system maintenance [105]. Sensors and biosensors detecting PSA, IL-6, IL-8, MMP, α-fetoprotein, CEA and CA-125 have been fabricated recently, as shown in Table 2.

PSA is the most commonly used tumour marker to diagnose prostate cancer, in terms of its concentration in blood, at levels greater than 4.0 ng mL^{-1} (Table 3). Various biosensors have been proposed for the detection of PSA in serum samples, as shown in Table 2. For example, Yang et al. [55] and Li et al. [56] used electrochemical immunosensors to detect PSA in human serum samples, by functionalizing graphene sheets with CdS quantum dots and cobalt hexacyanoferrate nanocomposites, respectively, to immobilize antibodies. Yang et al. [55] obtained a greater LOD (0.003 ng mL^{-1}) and wider linear range (0.005–10 ng mL^{-1}) compared to those obtained by Li et al. [56], 0.01 ng mL^{-1} and 0.01–2 ng mL^{-1}, respectively. Fig. 1 shows a transmission electron microscopy (TEM) image of graphene sheets (Fig. 1i), with a transparent and paper-like structure, and a TEM image of graphene sheets functionalized with quantum dots (Fig. 1ii), with a large number of quantum dots on the surface of graphene sheets [55]. In Fig. 1iii, the ultraviolet–visible (UV–Vis) spectra of graphene sheets (curve a), quantum dots (curve b) and quantum dot–graphene sheets (curve c) are depicted. No absorption peak was noted for graphene sheets. However, two absorption peaks were observed around 250 and 440 nm for pure quantum dots, and the two peaks shifted to 240 and 400 nm for quantum dots anchored onto graphene sheets [55]. In addition, Fig. 1iv compares the analytical response of the immunosensor using square wave voltammograms of the quantum dots on bare and graphene-modified electrodes. The peak current (at –0.8 V) was found to be three times greater with the graphene-modified

Table 2
Analytical parameters of clinical sensors and biosensors recently used for cancer and cardiac biomarkers

Analyte detected (matrix)	Sensor type	Linear range	LOD[a]	Sensitivity (slope)	Additional information	References
CANCER BIOMARKERS						
PSA (serum samples)	Electrochemical immunosensor based on CdS quantum dot-functionalized graphene sheets	0.005–10 ng mL^{-1}	0.003 ng mL^{-1}		RSD = 7.9%; n = 5	[55]
PSA (serum samples)	Electrochemical immunosensor based on graphene–Co hexacyanoferrate nanocomposites (GCE)	0.02–2 ng mL^{-1}	0.01 ng mL^{-1} (S/N = 3)		RSD = 6.7%; n = 5	[56]
PSA (serum samples)	Electrochemical immunosensor based on antibody-modified paramagnetic microparticles (screen-printed 8-sensor arrays based on 8 graphite working electrodes)	0–20 ng mL^{-1}	1.4 ng mL^{-1} ($3y_0$+s)	0.05 μA ng^{-1} mL^{-2}	RSD = 8%; n = 5 r^2 = 0.995	[57]
PSA (serum samples)	Electrochemical immunosensor based on MCWNT (SPCE)	0.005–4 ng mL^{-1}	0.005 ng mL^{-1}	0.077 μA pg^{-1} mL^{-2}	r^2 = 0.97	[58]
PSA (serum samples)	Electrochemical immunosensor based on Au nanoparticles–MWCNT–cross-linked starch nanocomposites (GCE)	0.01–0.5 ng mL^{-1}	0.007 ng mL^{-1} (S/N = 3)	63.94 μA ng^{-1} mL^{-2}	RSD = 4.1%; n = 6 r^2 = 0.9936 Recovery = 91.0–106.3%	[59]
PSA (serum samples)	Electrochemical immunosensor based on graphene and Ag-hybridized mesoporous silica nanoparticles (GCE)	0.01–10 ng mL^{-1}	0.002 ng mL^{-1}	3.6807 μA ng^{-1} mL^{-2}	RSD = 6.4%; n = 5 r^2 = 0.9963 Recovery = 97.0–102.5%	[60]
IL-8 (serum samples)	Electrochemical immunosensor based on MCWNT (SPCE)	8–1000 pg mL^{-1}	8 pg mL^{-1}			[58]
IL-8 (serum samples)	Electrochemical immunosensor based on superparamagnetic particles and Au nanoparticles	0–2000 pg mL^{-1}	0.001 pg mL^{-1}	0.0543 nA pg^{-1} mL^{-2}	r = 0.9782	[61]
IL-6 (serum samples)	Electrochemical immunosensor	0.01–1.3 pg mL^{-1}	0.01 pg mL^{-1}		r = 0.9914	[62]
IL-6 (serum samples)	Electrochemiluminescence immunosensor based on graphene oxide nanosheet/polyaniline nanowire/CdSe quantum dot nanocomposites (GCE)	0.5–10,000 pg mL^{-1}	0.17 pg mL^{-1}		RSD = 5.9%; n = 3	[63]
IL-6 (serum, urine, and saliva samples)	Electrochemical magnetoimmunosensor based on carboxyl-functionalized magnetic microparticles (SPCEs)	1.75–500 pg mL^{-1}	0.39 pg mL^{-1} ($3y_0$+s)	336 nA pg^{-1} mL^{-2}	RSD = 6.9–8.1%; n = 8 r = 0.999 Recovery = 98–103%	[64]
IL-6 (serum samples)	Electrochemical immunosensor based on Au–Pd–Ag nanoparticles (electrically heated carbon electrode)	0.1–100,000 pg mL^{-1}	0.059 pg mL^{-1} (S/N = 3)		RSD = 6.3%	[65]
IL-6 (serum samples)	Electrochemical immunosensor based on Au nanoparticle–graphene–silica sol–gel (ITO)	1–40 pg mL^{-1}	0.3 pg mL^{-1} (S/N = 3)	20.4 nA pg^{-1} mL^{-2}	RSD = 7.2%; n = 3 r = 0.9919	[66]
MMP-2 (serum samples)	Electrochemical immunosensor based on Au nanoparticles and nitrogen-doped graphene composites (GCE)	0.5–50,000 pg mL^{-1}	0.11 pg mL^{-1} (S/N = 3)	4.20 μA ng^{-1} mL^{-2}	RSD = 5.7% r = 0.997	[67]
MMP-2 (serum samples)	Optical biosensor based on graphene oxide	10,000–150,000 pg mL^{-1}	2500 pg mL^{-1}		RSD = 0.53–4.56% Recovery = 93.6–98.8%	[68]
MMP-3	Electrochemical immunosensor based on graphene oxide/polypyrrole ionic liquid nanocomposite (ITO)	1–1000 pg mL^{-1}	1 pg mL^{-1}			[69]
α-fetoprotein (serum samples)	Electrochemical magnetoimmunosensor based on Fe_3O_4/ZrO_2/nano-Au composite (GCE)	0.05–10 ng mL^{-1}	0.01 ng mL^{-1} (S/N = 3)	0.2906 μA ng^{-1} mL^{-2}	RSD = 2.5% r = 0.9905	[70]
α-fetoprotein (serum samples)	Photoelectrochemical immunosensor based on CdTe quantum dot–glucose oxidase bioconjugate (ITO)	0.0005—10,000 ng mL^{-1}	0.00013 ng mL^{-1}	4.60 μA ng^{-1} mL^{-2}	RSD = 0.8–1.5%; n = 5 r = 0.9997	[71]
α-fetoprotein (serum samples)	Electrochemical sensor based on MWCNT and Au nanoparticles	0.0005–100 ng mL^{-1}	0.00015 ng mL^{-1} (S/N = 3)		RSD = 2.7–5.1% r = 0.9969	[72]
α-fetoprotein (serum samples)	Electrochemical immunosensor based on Au and Ag nanoparticles (SPCE)	0.005–5.0 ng mL^{-1}	0.0039 ng mL^{-1} (S/N = 3)		CV = 5.3–7.9%; n = 5 r = 0.9954	[73]
α-fetoprotein (serum samples)	Electrochemical immunosensor based on mesoporous silica nanoparticles with Fe_3O_4 nanoparticles (GCE)	0.01–25 ng mL^{-1}	0.004 ng mL^{-1} (S/N = 3)		RSD = 1.8–3.5%; n = 5	[74]
CEA (serum samples)	Electrochemical immunosensor based on CNT/Au nanoclusters (GCE)	0.1–2.0 ng mL^{-1}	0.06 ng mL^{-1} (S/N = 3)	4.69 μA ng^{-1} mL^{-2}	CV = 5.6%; n = 5 r = 0.992	[75]

(*continued on next page*)

Table 2 (*continued*)

Analyte detected (matrix)	Sensor type	Linear range	LOD[a]	Sensitivity (slope)	Additional information	References
CEA (serum samples)	Electrochemical immunosensor based on chitosan–ferrocene and nano-TiO_2 film and Au nanoparticle–graphene nanohybrid	0.01–80 ng mL^{-1}	0.0034 ng mL^{-1} (S/N = 3)	0.5289 μA ng^{-1} mL^{-2}	RSD = 2.5%; n = 5 r = 0.9991	[76]
CEA (serum samples)	Electrochemical immunosensor based on Au nanoparticle–thionine–reduced graphene oxide nanocomposite film (GCE)	0.01–0.5 ng mL^{-1}	0.004 ng mL^{-1} (S/N = 3)	4.2 μA ng^{-1} mL^{-2}	RSD = 4.6%; n = 5 r = 0.9978 Recovery = 92.5–113.0%	[77]
CEA (serum samples)	Electrochemical sensor based on MWCNT and Au nanoparticles	0.0005–100 ng mL^{-1}	0.00002 ng mL^{-1} (S/N = 3)		RSD = 1.9–5.8% r = 0.9954	[72]
CEA (serum samples)	Electrochemical immunosensor based on MWCNT (μPAD)	0.05–50 ng mL^{-1}	0.01 ng mL^{-1}	2.587 μA ng^{-1} mL^{-2}	RSD = 4.2%; n = 10 r = 0.9964	[78]
CEA (serum samples)	Electrochemical immunosensor based on Au and Ag nanoparticles (SPCE)	0.005–5.0 ng mL^{-1}	0.0035 ng mL^{-1} (S/N = 3)		CV = 4.7–5.9%; n = 5 r = 0.9975	[73]
CEA (serum samples)	Electrochemical immunosensor based on Nafion membrane–SiO_2 nanoparticles (GCE)	0.000001–0.1 ng mL^{-1}	0.000001 ng mL^{-1} (S/N = 3)	0.10016 μA fg^{-1} mL^{-2}	RSD = 3.5%; n = 3 r^2 = 0.9944	[79]
CEA (serum samples)	Electrochemical immunosensor based on nano-Au-functionalized mesoporous carbon foam (GCE)	0.00005–1 ng mL^{-1}	0.000024 ng mL^{-1} (S/N = 3)		RSD = 7.6%; n = 3 r = 0.9997	[80]
CEA (serum samples)	Electrochemical immunosensor based on Au–Ag bimetallic nanoparticles (paper working electrode)	0.001–50 ng mL^{-1}	0.0003 ng mL^{-1} (S/N = 3)	15.58 μA ng^{-1} mL^{-2}	RSD = 5.1%; n = 11 r = 0.9965	[81]
CA 125 (serum samples)	Electrochemical immunosensor based on MWCNT (μPAD)	0.001–75.0 U mL^{-1}	0.2 U mL^{-1}	1.285 μA U^{-1} mL^{-2}	r = 0.9968	[78]
CA 125 (serum samples)	Electrochemical sensor based on MWCNT and Au nanoparticles	0.0001–100 U mL^{-1}	0.000037 U mL^{-1} (S/N = 3)		RSD = 3.6–5.9% r = 0.9965	[72]
CARDIAC BIOMARKERS						
CRP (serum samples)	Electrochemical immunosensor based on aldehyde-terminated nanocrystalline diamond	1–1000 nM	10 nM			[82]
CRP (serum samples)	Electrochemical immunosensor based Fe_3O_4–Au magnetic nanoparticles (SPCE)	1.2–200 ng mL^{-1}	0.5 ng mL^{-1}			[83]
CRP	Electrochemical immunosensor based on ZnO nanotubes	10–1000000 ng L^{-1}	0.0010 ng mL^{-1}	13.17 mV mg^{-1} L^{-1}	RSD < 5%; n = 6 r^2 = 0.99	[84]
CRP (serum samples)	Electrochemical magnetoimmunosensor based on carboxylic acid-modified magnetic beads (gold SPE)	0.07–1000 ng mL^{-1}	0.021 ng mL^{-1} (3s/m)	0.203 μA ng^{-1} mL^{-2}	RSD = 6.5%; n = 9 r = 0.997	[85]
CRP (serum samples)	Electrochemical immunosensor (polycrystalline Au electrodes)	60000–6000000 ng L^{-1}	19000 ng mL^{-1} (S/N = 3)			[86]
CRP (serum samples)	Piezoelectric immunosensor based on Fe_3O_4–SiO_2 magnetic nanoprobes	0.001–100 ng mL^{-1}	0.0003 ng mL^{-1}	30.1 Hz pg^{-1} mL^{-2}	CV = 2.4%; n = 5 r = 0.9943 Recovery = 86.7–107.0%	[87]
CRP (serum and saliva samples)	Electrochemical immunosensor based on SWCNT	0.1–100000 ng mL^{-1}	0.1 ng mL^{-1}		CV = 1.0–9.4%; n = 3 r^2 = 0.9924	[88]
CRP (serum samples)	Electrochemical magnetoimmunosensor based on carboxylic acid-modified magnetic beads (SPCE)	2–100 ng mL^{-1}	0.47 ng mL^{-1} (3s/m)	0.386 μA ng^{-1} mL^{-2}	RSD = 6.3%; n = 10 r = 0.996	[89]
NT-proBNP	Electrochemical immunosensor with Au and MWCNT composite	0.02–100 ng mL^{-1}	0.006 ng mL^{-1} (S/N = 3)	2.023 μA ng^{-1} mL^{-2}	RSD = 3.4%; n = 10 r = 0.997	[90]
NT-proBNP (serum samples)	Electrochemical magnetoimmunosensor based on avidin-functionalized magnetic nanoparticles	0.04–2.5 ng mL^{-1}	0.03 ng mL^{-1} (S/N = 3)		r = 0.9827	[91]
NT-proBNP (serum samples)	Electrochemical magnetoimmunosensor based on carboxylic acid-modified magnetic beads (SPE)	0.12–42.9 ng mL^{-1}	0.02 ng mL^{-1}		RSD = 9.7%; n = 9	[92]
NT-proBNP (serum samples)	Electrochemical magnetoimmunosensor based on carboxylic acid-modified magnetic beads (SPCE)	2–100 ng mL^{-1}	0.47 ng mL^{-1} (3s/m)		RSD = 9.4%; n = 10 Recovery = 105–111%	[89]
cTnT (serum samples)	Piezoelectric immunosensor based on Au nanoparticles	0.003–0.5 ng mL^{-1}	0.0015 ng mL^{-1}	63.82 Hz ng^{-1} mL^{-2}	CV = 7%; n = 5 r = 0.989	[93]
cTnT (serum samples)	Electrochemical immunosensor based on carboxylated CNT	0.1–10 ng mL^{-1}	0.033 ng mL^{-1}		CV = 3.7%; n = 10 r = 0.9996	[94]
cTnT (serum samples)	Electrochemical immunosensor based on amine-functionalized CNT (SPE)	0.0025–0.5 ng mL^{-1}	0.0035 ng mL^{-1} (3s/m)	3.25 μA ng^{-1} mL^{-2}	RSD = 3.8%; n = 7 r = 0.995	[95]
cTnT (serum samples)	Electrochemical immunosensor based on *o*-aminobenzoic film	0.05–5.0 ng mL^{-1}	0.016 ng mL^{-1} (3s/m)		RSD = 6.2%; n = 6 r = 0.992	[96]

(*continued on next page*)

Table 2 (*continued*)

Analyte detected (matrix)	Sensor type	Linear range	LOD[a]	Sensitivity (slope)	Additional information	References
cTnI	Electrochemical immunosensor based on Au nanoparticles (ITO)	1–100 ng mL^{-1}				[97]
cTnI	Electrochemical immunosensor (SPE)	1–100 ng mL^{-1}		5.5 μA ng^{-1} cm^{-2}	r = 0.987	[98]
cTnI	Electrochemical immunosensor based on Pt nanoparticles and graphene composite (GCE)	0.01–10 ng mL^{-1}	0.0042 ng mL^{-1} (S/N = 3)		RSD = 4–11%; n = 3 r = 0.991	[99]
cTnI (serum samples)	Optical immunosensor (fluorescence)	0–50 ng mL^{-1}	0.05 ng mL^{-1}		RSD = 7.5%; n = 6 r^2 = 0.9984	[100]
Myoglobin (plasma samples)	Electrochemical immunosensor based on Au nanoparticles	10–400 ng mL^{-1}	5 ng mL^{-1} (S/N = 3)		RSD = 15%; n = 3 r = 0.981	[101]
Myoglobin	Electrochemical immunosensor based on liquid crystal and Au nanoparticles (GCE)	9.96–72.8 ng mL^{-1}	6.29 ng mL^{-1} (3s/m)		RSD = 4.3%; n = 5 Recovery = 99.7–109.1%	[102]
Myoglobin (serum samples)	Optical immunosensor (SPR)	100–1000 ng mL^{-1}	31.0 ng mL^{-1} (S/N = 3)		CV = 4.9% r^2 = 0.99	[103]
Myoglobin (serum samples)	Optical immunosensor (fluorescence)	0–340 ng mL^{-1}			RSD = 2.3%; n = 6 r^2 = 0.979	[100]

CA 125: cancer antigen 125; CEA: carcinoembryonic antigen; CNT: carbon nanotubes; CRP: C-reactive protein; cTnI: cardiac troponin I; cTnT: cardiac troponin T; CV: coefficient of variation; GCE: glassy carbon electrode; IL-6: interleukin-6; IL-8: interleukin-8; ITO: indium tin oxide electrode; LOD: limit of detection; MMP-2: matrix metalloproteinase-2; MMP-3: matrix mettaloproteinase-3; MWCNT: multiwalled carbon nanotubes; NT-proBNP: amino-terminal pro-brain natriuretic peptide; PSA: prostate-specific antigen; RSD: residual standard deviation; SPCE: screen-printed carbon electrode; SPE: screen-printed electrode; SPR: Surface Plasmon Resonance; SWCNT: single-walled carbon nanotubes; μPAD: microfluidic paper-based analytical device.

[a] Determination of LOD: "S/N = 3": LOD is three times the signal-to-noise ratio; "3s/m": LOD is 3 times the standard deviation (s)/slope of calibration plot (m); "$3y_0$+s": LOD is 3 times the blank response (y_0) plus the standard deviation (s).

electrode than with the bare electrode (only with quantum dots), exhibiting an acceptable response for further biosensing of PSA.

According to Yang et al. [55], graphene sheets offer a very large surface area for the immobilization of several quantum dots, thus increasing the sensitivity of the immunosensor. In addition, the authors attributed the low LOD to the large amount of antibodies immobilized to the graphene sheet-modified electrode and the good conductivity of the graphene sheets, which in turn increased the sensitivity of Cd^{2+} (from the CdS quantum dots). The immunosensor successfully detected PSA in serum samples, as the PSA contents were compatible with the enzyme-linked immunosorbent assay (ELISA) measurement (a correlation coefficient of 0.898 was found between the PSA contents obtained by these two methods). Thus, this immunosensor can be used for routine clinical testing. Yang et al. [55] and Li et al. [56] also determined the selectivity of immunosensors by investigating their responses towards human IgG, BSA, lysozyme, vitamin C and glucose. Both groups tested 1 ng mL^{-1} of PSA solution containing 100 ng mL^{-1} of interfering substances. They showed that the current variation due to interfering substances was less than 8% of the current measured in the absence of the interfering compounds. This indicates the good selectivity of both immunosensors. Based on the analytical performance of the biosensors reported in Table 2 in detecting PSA, Zani et al. [57] obtained the highest LOD (1.4 ng mL^{-1}). They [57] developed an electrochemical immunosensor based on protein G-coated paramagnetic microparticles modified with antibodies specific to PSA. These microparticles were immobilized on screen-printed graphite 8-sensor arrays as working electrodes, which functioned as multiplexed electrochemical platforms. Recently, Li et al. [60] fabricated an electrochemical immunosensor based on graphene (functionalized with ferrocene–carboxaldehyde composites) and silver-hybridized mesoporous silica nanoparticles immobilized on glass carbon electrodes to detect PSA in serum samples. They obtained a low LOD (0.002 ng mL^{-1}) possibly because mesoporous silica materials were used, which have large specific surface area, uniform structure and controlled pore size [60]. The immunosensor exhibited good stability (RSD lower than 10% after three weeks of standby) and reproducibility (RSD of 6.4%). This indicates that the structure of the nanocomposites can facilitate the immobilization of biomolecules other than PSA useful in clinical diagnostics [60]. According to the authors, the silver nanoparticles amplified the signal and in turn the sensitivity of electrochemical immunosensors due to their biocompatibility and high electrical conductivity. Li et al. [60] tested five different concentrations of PSA (1.0, 2.0, 4.0, 6.0 and 8.0 ng mL^{-1}) in human serum samples (without any treatment) via the standard addition method, with recoveries of 97.0–102.5% and RSD below 5.4%. Thus, they showed that this immunosensor can be applied to clinical practice. In addition, the analytical results of the immunosensor were compared with those of a commercial ELISA, and RSDs ranging from –4.61% to 4.10% were obtained between the two methodologies. Thus, immunosensors can be considered for clinical application [60]. To determine selectivity, the immunosensor was incubated in 2 ng mL^{-1} of PSA solution containing 200 ng mL^{-1} of interfering substances (hIgG, lysozyme and α-fetoprotein). The current variation due to interfering substances was less than 5.2% of that without interferences. This indicated that the selectivity of the immunosensor was good [60].

Interleukins, which belong to the cytokine family, play a key role in the inflammatory response of diseases such as psoriasis, rheumatoid arthritis, cardiovascular disease (CVD) and inflammatory bowel disease, as well as diabetes and Alzheimer's disease [64,66]. For example, IL-6 is a useful biomarker overexpressed in several types

Table 3
Normal values of cancer and cardiac biomarkers in human blood

Analyte	Normal value	Reference
CANCER BIOMARKERS		
PSA	4.0 ng mL^{-1}	[60]
IL-6	6 pg mL^{-1}	[64]
IL-8	13–20 pg mL^{-1}	[61]
MMP-2	367–770 ng mL^{-1}	[104]
MMP-3	15–72 ng mL^{-1}	[104]
α-fetoprotein	<20 ng mL^{-1}	[70]
CEA	5 ng mL^{-1}	[78]
CA-125	35 U mL^{-1}	[78]
CARDIAC BIOMARKERS		
CRP	3 mg L^{-1}	[82]
NT-proBNP	1 ng mL^{-1}	[89]
cTnT	0.3 ng mL^{-1}	[93]
cTnI	0.01–0.1 ng mL^{-1}	[99]
Myoglobin	50–100 ng mL^{-1}	[100]

of cancer such as prostate cancer or head and neck squamous cell carcinoma, with the serum concentrations increasing up to the nanogram per millilitre range. The IL-6 level in the serum of healthy individuals is about 6 pg mL^{-1} (Table 3). The traditional analytical techniques used to detect IL-6 include ELISA, fluorescent microarray, chemiluminescence immunoassay, biosensors based on fluorescence and conductimetry [65]. Other current biosensors are based on electrochemistry, as shown in Table 2. For example, Liu et al. [63] reported an immunosensor based on electrochemical and optical principles, with graphene oxide nanosheets, polyaniline NWs and CdSe quantum dot nanocomposites immobilized on glass carbon electrodes, to detect IL-6 in serum samples. The immunosensor exhibited long-term stability as the analytical response did not change significantly when the sensor was stored for 14 days at 4°C. An RSD of 7.4% and good reproducibility were reported, because the detection of 10 pg mL^{-1} of IL-6 in five independent sensors provides an RSD of 7.6%. In addition, the analytical results of the immunosensors were compared with those of ELISA methodology, and relative deviations from –5.84% to 6.21% were found between the two methodologies, which indicates the applicability of the sensor to the determination of IL-6 levels in human samples [63]. The nanocomposite showed excellent biocompatibility, dispersability and solubility, which can improve the electrochemiluminescence biosensing method used to detect IL-6 in serum samples or other proteins in clinical samples [63]. Liu et al. [63] also demonstrated that the proposed immunosensor has sufficient selectivity for IL-6 detection, which could differentiate IL-6 from its analogues in complex samples. This is confirmed by the acceptable RSD (6.3%) obtained on comparing the response for IL-6 with that for BSA, CEA and hIgG. Recently, Wang et al. [66], Ojeda et al. [64] and Lou et al. [65] proposed electrochemical biosensors for the detection of IL-6 in serum samples (Table 2), based on gold nanoparticles/graphene/silica sol–gel, carboxyl-functionalized magnetic microparticles and gold/palladium/silver nanoparticles, respectively. In the first two works, similar LODs were obtained (0.3 and 0.39 pg mL^{-1}) but with Ojeda et al. [64] obtaining a wider linear range (1.75–500 pg mL^{-1}) and better sensitivity (336 nA pg^{-1} mL^{-1}, respectively) than Wang et al. [66], about 1–40 pg mL^{-1} and 20.4 nA pg^{-1} mL^{-1}, respectively. Wang et al. [66] used an indium tin oxide (ITO) electrode, with the gold nanoparticles/graphene/silica sol–gel film being synthesized in situ. This offered a stable network for the labelling of the gold nanoparticles/polydopamine/CNT composite used to immobilize antibodies specific to IL-6. Polydopamine is a novel, simple, inexpensive, 'green' and stable material, and its association with gold nanoparticles and CNT is promising in clinical diagnosis [66]. In addition, Wang et al. [66] found that the results for their sensor were in line with those for the reference ELISA methodology, as a correlation coefficient of 0.990 was found between the two methodologies, which indicates the applicability of the fabricated immunosensor in bioelectronic systems. The immunosensor was found to have acceptable selectivity as reflected by the variation of 2.2–8.8% in the response of the immunosensor to interfering analytes (α-fetoprotein, human chorionic gonadotropin and PSA) [66]. Ojeda et al. [64] showed that the fabricated exhibits excellent storage stability because of the anti-IL-6–magnetic bead conjugates, which provide amperometric responses with no significant loss for at least 36 days. In addition, the analytical results obtained with the biosensor were statistically in agreement with those for a commercial ELISA kit, as no significant difference was found between the two methodologies (at $\alpha = 0.05$). Compared to the first two groups, Lou et al. [65] reported a lower LOD (0.059 pg mL^{-1}) and a wider linear range (0.1–100,000 pg mL^{-1}) for their electrochemical immunosensor. Lou et al. [65] applied a competitive dual signal amplification strategy by combining the electrically heated carbon electrode technique with gold nanoparticles. According to the authors, the electrically heated carbon

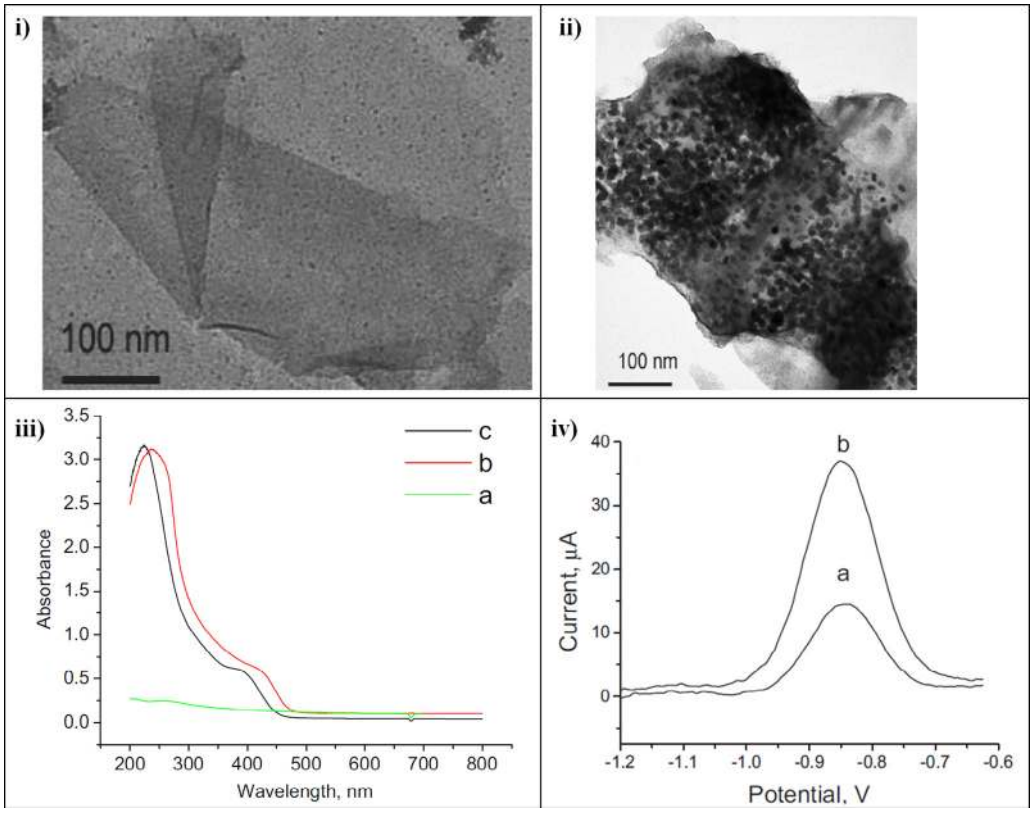

Fig. 1. **i**) TEM image of graphene sheets; **ii)** TEM image of graphene sheets functionalized with quantum dots; **iii)** UV–Vis spectra of a) graphene sheets, b) quantum dots and c) quantum dot–graphene sheets; and **iv)** Square wave voltammogram response of electrodes with a) only quantum dots and b) electrodes with quantum dots in graphene sheets (Reprinted from Yang et al. [55], with permission from Elsevier).

electrode technique accelerates the reaction kinetics without changing the bulk solution temperature. Thus, the mass transport is enhanced by changing the temperature of the electrode. In turn, the electrochemical signal is enhanced together with a higher signal-to-background ratio, which leads to the high analytical performance. With respect to its stability, more than 90% of the initial responses for IL-6 were obtained when the biosensor was stored for 14 days at 4°C; this is due to the good biocompatibility of retaining the bioactivity of proteins. In addition, the immunosensor was tested to detect IL-6 in serum samples, the results of which were compared with those obtained for the ELISA methodology. An RSD less than 6.3% was reported for eight individual biosensors for 100 pg mL^{-1} of IL-6, suggesting its potential application towards the early evaluation of tumour diseases [65]. The selectivity of the immunosensor was also tested, with no significant differences (RSD from 6.5% to 10.9%) being observed when 10 pg mL^{-1} IL-6 was mixed with 100 pg mL^{-1} of BSA, cTnI, CEA and MMP-2. Thus, these analytes did not interfere notably in the functioning of the immunosensor [65]. Tang et al. [62] proposed another electrochemical immunosensor to detect IL-6 in serum samples. It is based on the microfluidic principle, providing an LOD in the femtogram per millilitre range (10 fg mL^{-1}, that is, 0.01 pg mL^{-1}) and a linear range of 10–1300 fg mL^{-1} (0.01–1.3 pg mL^{-1}). Thus, it is an excellent candidate for the detection of other biomarkers for cancer diagnostics. According to Tang et al. [62], microfluidics offered excellent control of mass transport, enhanced signal-to-noise ratio and increased portability. In addition, the major advantage of microfluidics is the low cost of the sensors, which produces high-quality microchips with a minimal sample volume of 1 μL required [62]. The schematic representation of the microfluidic chips proposed by Tang et al. [62] is shown in Fig. 2.

According to Tang et al. [62], the microfluidic array is a very promising cheap, disposable, chip-based diagnostic tool for early cancer detection and monitoring. The very low LOD allows extensive dilution of samples and in turn minimizes the non-specific binding of potentially interfering biomolecules in serum. Thus, these arrays can be used to test for cancer recurrence.

The MMP family of zinc-dependent endopeptidases are essential for the regulated degradation and processing of extracellular matrices, while also facilitating host and tumour communication [67]. For example, MMP-2 is a key MMP in tumour growth, invasion and metastasis, involved in physiological and pathological states including morphogenesis, reproduction and tissue remodelling [67]. MMP-3 can also be used to diagnose and monitor such diseases, as it elevated expression is associated with head and neck squamous cell carcinoma and adrenal tumours [61]. In Table 2, three works on the detection of MMP-2 and MMP-3 with different biosensors are listed. For MMP-2, Yang et al. [67] developed an electrochemical immunosensor based on gold nanoparticles and nitrogen-doped graphene composite immobilized on a glass carbon electrode, whereas Song et al. [68] constructed an optical biosensor based on graphene oxide. According to Song et al. [68], graphene oxide has been used to develop biosensors based on fluorescence resonance energy transfer, because of its superior fluorescence quenching capacity and unique adsorption characteristics for biomolecules. The LOD (0.11 pg mL^{-1}) of an electrochemical immunosensor proposed by Yang et al. [67] was superior to the LOD of an optical biosensor (2500 pg mL^{-1}) obtained by Song et al. [68]. Moreover, the immunosensor showed a wide linear range (0.5–50,000 pg mL^{-1}) with high selectivity and long-term stability (90% of the initial response persisted after storing the biosensors at 4°C for week), which can thus be used to satisfactorily detect proteins in clinical laboratories [67]. In addition, the analytical results of the immunosensors were compared with those of an ELISA methodology, which were found to be in agreement, with relative deviations ranging from –5.97% to 2.94%. This indicated the applicability of the immunosensor to determining MMP-2 levels in human plasma [67]. The authors also listed the advantages of the composite of gold nanoparticles and nitrogen-doped graphene sheet for biosensing. This composite facilitates robust immobilization of antibodies, promotes electron transfer and exhibits excellent electrochemical activity, thus enhancing the analytical performance of the immunosensor due to the homogeneous dispersion of gold nanoparticles on the nitrogen graphene sheet.

The α-fetoprotein, an oncofetal glycoprotein, is the most important and widely use liver cancer tumour marker. It is mainly produced by the liver, yolk sac and gastrointestinal tract of a human fetus; its increased levels in adult serum indicate hepatocellular carcinoma or endodermal sinus tumour [71]. Conventional techniques for the detection of α-fetoprotein include ELISA, electrochemistry, electrochemiluminescence, mass spectrometry, QCM and SPR immunoassays. However, their limitations include relatively sophisticated instrumentation, significant sample volume, limited sensitivity and clinically unrealistic cost and time. Thus, new, simple and inexpensive methods have been proposed for the detection of α-fetoprotein or other biomarkers in the serum of both healthy and cancer patients [71]. Various electrochemical sensors have been proposed for the detection of α-fetoprotein in serum samples (Table 2), which use nanomaterials for signal transduction. Li et al. [71], Ge et al. [72], Lai et al. [73] and Gan et al. [70] used CdTe quantum dots,

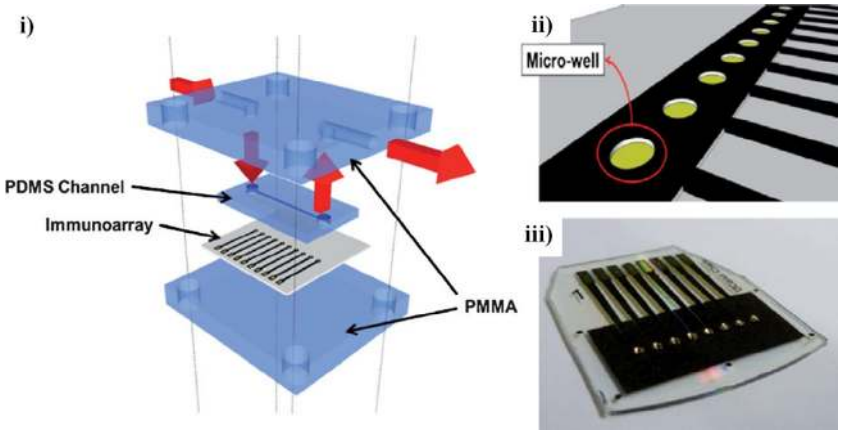

Fig. 2. i) Fitting the 8-electrode immunoarray into the microfluidic device. The array is sandwiched between two layers of poly(methylmethacrylate) (PMMA) and one layer of poly(dimethyl)siloxane (PDMS) acting as microfluidic channel above the sensor electrodes. The red arrows indicate the flow of buffer; **ii)** Computer-generated design of the gold array showing microwells around electrodes; and **iii)** Completed array of 8 electrodes with individual microwells containing 1 μL aqueous droplets (Reproduced from Tang et al. [63] with permission of The Royal Society of Chemistry).

MWCNT/gold nanoparticles, gold/silver nanoparticles and Fe_3O_4/ZrO_2/nanogold composites, with LODs of 0.00013, 0.00015, 0.0039 and 0.01 ng mL^{-1}, respectively. These different LODs can be attributed to the different transduction principles applied. All sensors are based on the electrochemical principle. However, Li et al. [71] and Gan et al. [70], respectively, combined the optical mechanism (exciting detection technique using quantum dots as photoactive materials) and magnetic mechanism (preparation of magnetic particles: Fe_3O_4–ZrO_2–Au–polylysine) with electrochemistry. Li et al. [71] reported good long-term stability of two weeks at 4°C as they found no apparent change in the photocurrent response on detecting 10 ng mL^{-1} of α-fetoprotein. Their immunosensors were found to be feasible for clinical application with relative deviations ranging from –3.6% and 3.0% compared with the ELISA results. Lai et al. [73] reported the same sensor stability (90% of initial response remained after two weeks at 4°C). Further, when human serum samples were tested for α-fetoprotein with the immunosensor and with a commercial electrochemiluminescence test, relative errors ranging from –10.5% to 8.5% were observed, indicating the good accuracy of the reported biosensor for clinical sample detection. The biosensor developed by Gan et al. [70] was found to be more stable, as no apparent change in response was observed with measurement of α-fetoprotein every 3–5 days, with RSD of 3.0% for 30 days (at 4°C). The authors attributed the good stability to the consistency of the Fe_3O_4–ZrO_2–Au–polylysine membrane and the firm attachment of protein molecules to the surface of the glass carbon electrode. The immunosensor can be used to determine α-fetoprotein levels in human serum, as the average concentration of α-fetoprotein with the biosensor (4.56 ng mL^{-1}) was similar to that obtained with ELISA (4.89 ng mL^{-1}), indicating no significant difference. In addition, Gan et al. [70] verified the good selectivity of their immunosensor for the determination of α-fetoprotein, as the sensor response for various analytes (100 ng mL^{-1} CEA, 1 μg mL^{-1} hIgG, 20 ng mL^{-1} carbohydrate antigen 19-9, 20 ng mL^{-1} human chorionic gonadotropin antigen, 2 μg mL^{-1} BSA, 2 μg mL^{-1} dopamine, 2 μg mL^{-1} L-lysine, 2.5 μg mL^{-1} uric acid, 2.5 μg mL^{-1} glucose, 5 μg mL^{-1} ascorbic acid and 5 μg mL^{-1} Na^+) did not interfere with the determination of 5.0 ng mL^{-1} of α-fetoprotein (signal dropped below 5%). Recently, Wang et al. [74] proposed an electrochemical immunosensor based on mesoporous silica nanoparticles, which were used as carriers to immobilize secondary antibodies as well as Fe_3O_4 nanoparticles and the enzyme horseradish peroxidase, both of which were used as signal amplification labels. The mesoporous silica nanoparticles are known to have a large specific surface area and good biocompatibility. Thus, they are promising candidates for use in electrochemical sensors [74], in addition to their lower cost compared with noble metal nanoparticles (Au, Al or Pt) often used in electrochemical sensors, as shown previously. For the electrochemical immunosensor (0.01–25 ng mL^{-1}), a good linear relationship was noted between the current change and concentrations of α-fetoprotein with a low LOD (0.004 ng mL^{-1}), which suggests the applicability of these immunosensors for the detection of other tumour markers [74]. In addition, compared to the analytical results for an ELISA methodology, the immunosensor showed relative deviations between –6.1% and 1.3% for the detection of α-fetoprotein in serum samples, indicating its suitability in real sample detection.

CEA, a glycoprotein, is the most extensively used tumour marker for clinical diagnosis of lung cancer, ovarian carcinoma, breast cancer and cystadenocarcinoma, with a cut-off value of 5 ng mL^{-1} [78,80]. The levels of CEA are elevated in the case of inflammation or tumours in any endodermal tissue including the gastrointestinal tract, respiratory tract, pancreas and breast [106]. Several analytical techniques based on immunoassays have been reported for the determination of CEA, including radioimmunoassays, enzyme immunoassays and fluoroimmunoassays. However, they are limited by radiation hazards, long analysis times or the need for qualified personnel and/or sophisticated instrumentation [107]. As early diagnosis and treatment of cancer are necessary, sensitive, precise and accurate analytical techniques must be developed for determining CEA with low concentration levels in complex biological samples [79]. For example, electrochemical biosensors have several advantages over the previously described molecular detection approaches, including the ability to analyse complicated body fluids, high sensitivity, compatibility with microfabrication technologies, low manpower requirements and compact instrumentation that is compatible with portable devices [107]. In Table 2, various electrochemical biosensors detecting CEA in serum samples are listed, with differing values of figures of merit such as linearity and sensitivity. For example, Han et al. [76], Kong et al. [77] and Lai et al. [73] fabricated electrochemical immunosensors for CEA based on different transduction materials. Han et al. [76] fabricated an electrochemical immunosensor based on chitosan–ferrocene, nano-TiO_2 film and gold nanoparticle–graphene nanohybrid. Kong et al. [77] proposed an electrochemical immunosensor based on gold nanoparticle–thionine–reduced graphene oxide nanocomposite films. Lai et al. [76] fabricated an electrochemical immunosensor based on gold and silver nanoparticles. Han et al. [76] and Kong et al. [77] obtained similar LODs (0.0034–0.004 ng mL^{-1}) but different sensitivities (4.2 and 0.53 μA ng^{-1} mL^{-2}, respectively) and linearity (0.01–80 ng mL^{-1} and 0.01–0.5 ng mL^{-1}, respectively), as shown in Table 2. Han et al. [76] used their biosensor to test real serum samples, with ELISA as the reference method. They found good agreement between both analytical methodologies, as the relative deviations of the biosensor results ranged from –8.31% to 7.58%. Kong et al. [77] performed recovery experiments via a standard addition method (CEA concentrations from 40 to 200 pg mL^{-1}) in human serum, which was then analysed with the proposed immunosensor. They achieved recovery in the range of 92.5–113.0%, thus indicating the feasibility of this immunosensor in determining CEA in human serum for routine clinical diagnosis. Wang et al. [79] developed a simple label-free electrochemical immunosensor based on Nafion membrane containing SiO_2 nanoparticles immobilized on glass carbon electrodes for the detection of CEA in serum samples. Wang et al. [79] obtained an excellent LOD in the femtomolar range (1 fg mL^{-1}, that is, 0.000001 ng mL^{-1}) with their immunosensor, with a linear response from 0.000001 to 0.1 ng mL^{-1}. In addition, the analytical results obtained with their immunosensor for detecting CEA in human serum samples are consistent with the data of a microparticle enzyme immunoassay, with relative errors of –8% to 5% [79]. The specificity of the immunosensor was also determined by mixing 1 ng mL^{-1} of CEA with 1 ng mL^{-1} of glucose, uric acid, α-fetoprotein, BSA, hIgG and ascorbic acid [79]. Wang et al. [79] verified that the variation in analytical response obtained from interference substances was less than 7.6% compared with that of pure CEA, indicating the good selectivity of the immunosensor. Recently, Lin et al. [80] and Sun et al. [81] constructed electrochemical immunosensors for the detection of CEA in serum samples based on the transduction principle. They used nanogold-functionalized mesoporous carbon foam (immobilized on glass carbon electrodes) and gold–silver bimetallic nanoparticles (immobilized on paper working electrodes), respectively, to immobilize the antibodies specific to CEA. As shown in Table 2, the LOD obtained in these two studies, together with that of Wang et al. [79], were the lowest compared to other works reporting the detection of CEA with electrochemical immunosensors. Lin et al. [80] proposed a method to amplify the immunosensor signal by incorporating a commercial silver enhancer solution, which is a mixture of silver and colloidal gold. According to the authors, this new amplification strategy is a very promising ultrasensitive electrochemical biosensing method, as reflected in the LOD. Lin et al. [80] obtained a better LOD (0.000024 ng mL^{-1}) than Sun et al. [81] did (0.0003 ng mL^{-1}), probably due to the signal transduction, which was amplified in the study by Lin et al. [80], thus enhancing the

stability of metal particles. In both studies, the results obtained with fabricated biosensors for the detection of CEA in real human serum samples were compared with reference methodologies, that is, commercial electrochemiluminescence tests. They were found to be in good agreement, with relative errors less than 11.9% and less than 3.2% obtained by Lin et al. [80] and Sun et al. [81], respectively.

Cancer antigen 125 (CA 125) is a serum cancer biomarker used to monitor and follow up ovarian, breast and uterine cancer patients. It is also used for the prognosis of response to various cancer therapies [9]. Its cut-off value in clinical diagnosis is 35 U mL^{-1} (Table 3). As listed in Table 2, Wang et al. [78] and Ge et al. [72] reported multiplexed electrochemical immunosensors based on MWCNTs, functionalized on a microfluidic paper-based analytical device (μPAD) denoted as wax-patterned microfluidic paper-based three-dimensional electrochemical devices (3D-μPED) and on MWCNT/gold nanoparticles (functionalized on an electrode array-based paper), respectively, with the ability to simultaneously detect more than one cancer biomarker in serum samples. Wang et al. [78] reported a simple, sensitive, low-cost, disposable and portable biosensor for the detection of CEA and CA 125, and Ge et al. [72] proposed a multi-analyte biosensor for the simultaneous detection of four cancer biomarkers (α-fetoprotein, CEA, CA 125 and CA 153) using electrode arrays with high throughput, low cost, small consumption, simple operation and high sensitivity. The schematic configurations and calibration curves obtained in the two works are shown in Fig. 3.

The multiplexed configuration can enhance the sample throughput, shorten the assay time and decrease the sample consumption and costs [72]. For both works, the calibration plots obtained for CA 125 and CEA showed a good linear relationship between the analytical response (peak currents) and the logarithm values of CA 125 and CEA concentration, with correlation coefficients of 0.9968 and 0.9964, respectively, as reported by Wang et al. [78], and correlation coefficients of 0.9965 and 0.9954, respectively, for CA 125 and CEA, as reported by Ge et al. [72] (Table 2). For both CEA and CA 125, Ge et al. [72] obtained a better LOD (0.00002 ng mL^{-1} and 0.000037 U mL^{-1}, respectively) than Wang et al. did [78] (0.01 ng mL^{-1} and 0.2 U mL^{-1}, respectively). However, both biosensors exhibited linear ranges covering most levels in human serum (Table 2). MWCNTs exhibit high chemical stability, good electrical conductivity and strong adsorptive ability. Moreover, their high surface area provides a large loading capacity for nanoparticles, thus improving catalytic activity when metal nanoparticles are supported on MWCNTs [108]. This effect was demonstrated in the biosensor fabricated by Ge et al. [72], with the MWCNTs acting as heterogeneous catalyst supports for gold nanoparticles. Wang et al. [78] and Ge et al. [72] developed sensors to detect CA 125 and CEA in human serum samples. The analytical results were compared with those of a reference methodology (commercial electrochemiluminescence method). Wang et al. [78] obtained relative errors between the sensor and the reference method below 5.8% for CA 125 and below 6.5% for CEA. Ge et al. [72] obtained RSDs between 2.5% and 5.9% for CA 125 and between 1.4% and 6.3% for CEA, which were in good agreement between the two methodologies and for both works.

4.1.2. Cardiac biomarkers

CVDs such as cerebral vascular accident and coronary heart disease are among the major causes of ill health, invalidity and death worldwide [109]. Thus, determining specific blood compounds (biomarkers) has been suggested to identify high-risk patients in terms of CVD risk. Thus, early detection of cardiac biomarkers with high sensitivity is imperative in clinical diagnostics. Various analytical techniques have been used, such as turbidimetry, SPR and immunoassays. However, these techniques require pretreatment and labelling, and are time consuming, for use in practical clinical routine.

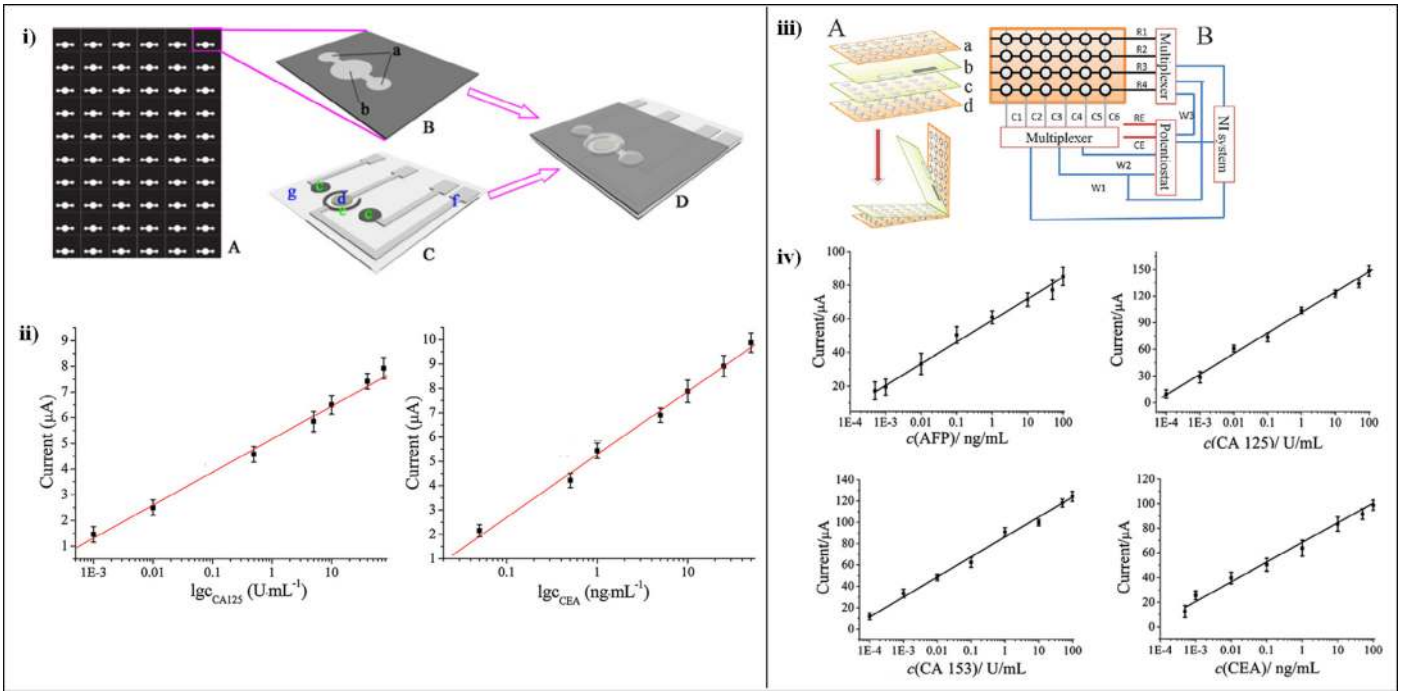

Fig. 3. **i)** Schematic representation of 3D-μPED. (A): wax-patterned paper sheet; (B): 3D-μPED [a) paper working zones and b) paper auxiliary zone]; (C): screen-printed electrodes [c) carbon working electrodes, d) Ag/AgCl reference electrode, e) carbon counter electrode, f) silver conductive channel and pad, and g) transparent polyethylene terephthalate substrate]; (D): after stacking, the paper working zones and the paper auxiliary zone will be aligned to the screen-printed working electrodes, counter electrode and reference electrode (Reprinted from Wang et al. [78], with permission from Elsevier); **ii)** Calibration curves for CA 125 and CEA (eleven measurements for each point) (Reprinted from Wang et al. [78], with permission from Elsevier); **iii)** (A) Layered structure of the device; (B) Schematic diagram of the addressable electrode array detection system [a) and d) polyethylene terephthalate substrates with column electrodes (C*n*) and row electrodes (R*n*); b) reference electrode (RE), c) sensing sites with column electrodes (W*n*) and counter electrode (CE)] (Reproduced from Ge et al. [72] with permission of The Royal Society of Chemistry); **iv)** Calibration curves for immunoassay of tumour markers (Reproduced from Ge et al. [72] with permission of The Royal Society of Chemistry).

Thus, biosensors have been considered for the rapid detection of cardiac biomarkers due to their miniaturization, portability, flexibility and sensitivity [86,87].

In Table 2, some recent works reporting biosensors for the detection of CRP, cardiac troponins, NT-proBNP and myoglobin in serum samples are listed. Most of these studies reported using nanomaterials or a combination of nanomaterials and composites, mainly due to their large surface area and good biocompatibility, which enhanced the analytical performance of these biosensors [87]. For example, Ibupoto et al. [84], Zhou et al. [87] and Justino et al. [88] ZnO nanotubes, Fe_3O_4–SiO_2 magnetic nanoprobes and SWCNTs as labels to immobilize antibodies in immunosensors for CRP detection. At levels exceeding 3 mg L^{-1}, CRP, an acute-phase protein, is used to evaluate the risk of developing CVDs such as atherosclerosis, angina, coronary heart disease, peripheral artery disease, myocardial infarction and stroke. It can also be used as a reliable marker for tissue injury, infection and inflammation [82]. Ibupoto et al. [84], Zhou et al. [87] and Justino et al. [88] reported low LODs, that is, 0.001, 0.0003 and 0.1 ng mL^{-1}, respectively, which were lower than those obtained with traditional immunoassays (30–200 ng mL^{-1}) [84,110]. All studies reported enhanced analytical performance with the immunosensors. The time response of the electrochemical immunosensor fabricated by Ibupoto et al. [84] was less than 10 seconds, which detected CRP with good reproducibility (RSD less than 5%) and stability (3 days). However, the immunosensor was not tested in real samples, which limits further clinical application. Ibupoto et al. [84] tested the proposed sensor in a solution with common interferents (glucose, urea, uric acid as well as sodium, potassium and iron ions) and observed a negligible response. Both the piezoelectric immunosensor and electrochemical immunosensor reported by Zhou et al. [87] and Justino et al. [88], respectively, were validated for the detection of CRP in serum and saliva samples. Zhou et al. [87] obtained good recoveries (87–107%) for the detection of CRP in various serum samples for the immunosensors and the classical ELISA methodology, as well as good reproducibility (CV of 2.4%) and repeatability (CV of 3.4%). Piezoelectric immunosensors offer major advantages such as allowing surface regeneration and repeated use (stability of analytical response of two weeks). Thus, they constitute a versatile analytical tool for the detection of CRP or other cardiac biomarkers. Justino et al. [88] list the advantages of electrochemical immunosensors as point-of-care devices for assessing CVD risk: these immunosensors are disposable, label-free, low cost and easy to analyse. The immunosensors were validated by analysing serum and saliva samples with the ELISA methodology, which showed comparable analytical performance. Linear correlations were found between the immunosensor and ELISA when applied to serum ($r^2 = 0.9904$) and saliva ($r^2 = 0.9991$) samples. Thus, the non-invasive sampling methodology reported by Zhou et al. [87] and Justino et al. [88] to detect CRP can be used to diagnose and monitor CVD. Recently, the group of Esteban-Fernández de Ávila [85,89] proposed two amperometric magnetoimmunosensors for the detection of CRP, both using carboxylic acid-modified magnetic beads as labels for the immobilization of antibodies. The first biosensor [85] was composed of disposable gold screen-printed electrodes to detect CRP in serum samples, whereas the second biosensor [89] comprised screen-printed carbon electrodes for the multiplexed detection of CRP and NT-proBNP, which is another cardiac biomarker (Table 2). According to Esteban-Fernández de Ávila et al. [85], magnetic beads have been useful used to construct electrochemical immunosensors to enhance their sensitivity, reduce the time of analysis and minimize matrix effects. Comparable sensitivity (0.203–0.386 μA ng^{-1} mL^{-2}) and reproducibility (RSD of 6.3–6.5%) were found with the CRP immunosensors but with LOD of different orders of magnitude: 0.021 ng mL^{-1} reported by Esteban-Fernández de Ávila et al. [85] and 0.47 ng mL^{-1} for the multiplexed immunosensor proposed by Esteban-Fernández de Ávila et al. [89]. Esteban-Fernández de Ávila et al. [85] stated that the low LODs were of practical advantage in the case of strong matrix effects for real clinical samples, which necessitates sample dilution prior to the analysis. Both immunosensors were successfully applied to spiked serum samples, which demonstrate the applicability of such sensing platforms for the clinical diagnosis of CRP. With the same multiplexed immunosensor, but for the detection of NT-proBNP, Esteban-Fernández de Ávila et al. [89] obtained a similar LOD to that for detecting CRP, but with lower reproducibility (9.4%). According to Esteban-Fernández de Ávila et al. [89], the low cost, ease of automation and miniaturization of multiplexed immunosensors, as well as the use of disposable mass-produced electrodes, make this approach a promising alternative tool for developing point-of-care devices for *in situ* clinical diagnosis. Another biomarker for predicting cardiac risk is NT-proBNP, with a key role in the natriuretic, diuretic and vasodilatory systems, as well as in the inhibition of the renin–angiotensin–aldosterone system and the sympathetic nervous system [91]. Zhuo et al. [90] and Yi et al. [91] also reported electrochemical immunosensors for the detection of NT-proBNP based on gold–MWCNT composites and avidin-functionalized magnetic nanoparticles, respectively (Table 2). Zhuo et al. [90] reported a better LOD (0.006 ng mL^{-1}) and a wide linear range (0.02–100 ng mL^{-1}) than Yi et al. [91] did, reporting an LOD of 30 pg mL^{-1} and a linear range of 0.04–2.5 ng mL^{-1}. The main advantage of the immunosensor proposed by Yi et al. [91] is the simple regeneration procedure, which includes washing the magnet with the buffer to remove the avidin-functionalized magnetic nanoparticles, antigen and antibodies.

Troponins are the most specific and sensitive biomarkers of myocardial cell injury. They, they have been used to test for acute myocardial infarction [96]. Troponins such as cTnT and cTnI can control the calcium-mediated interactions between actin and myosin in cardiac and skeletal muscles; cTnT is expressed in skeletal muscle to a lesser extent, whereas cTnI has not been identified outside of the myocardium [99]. Increased levels of cTnT (higher than 0.3 ng mL^{-1}) are highly specific to cardiac injury and are significantly associated with an increased risk of re-infarction and death, which facilities early diagnosis [93]. As shown in Table 2, Fonseca et al. [93], Gomes-Filho et al. [94], Silva et al. [95] and Mattos et al. [96] developed immunosensors based on gold nanoparticles, carboxylated CNTs, amine-functionalized CNTs and *o*-aminobenzoic films, respectively, for immobilizing antibodies specific to cTnT, with an LOD ranging from 0.0015 to 0.033 ng mL^{-1}. All immunosensors were used for serum samples with high sensitivity. They can be used for point-of-care diagnosis of acute myocardial infarction. For example, Gomes-Filho et al. [94] and Silva et al. [95] compared the cTnT concentrations obtained with both immunosensors in human serum samples to the levels obtained with electrochemiluminescence immunoassays. They [94,95] obtained correlation coefficients of 0.987 and 0.990 between the two methods ($p < 0.0001$), respectively. Recently, Singal et al. [99] and Cho et al. [100] reported electrochemical and optical immunosensors, respectively, for the detection of cTnI. The electrochemical immunosensor (based on impedance) was prepared with functionalized platinum nanoparticles immobilized on a graphene monolayer deposited on a glass carbon electrode, obtaining an LOD of 0.0042 ng mL^{-1} with reproducible results (RSD of 4–11%) and a linear range of 0.01–10 ng mL^{-1} [99]. Singal et al. [99] combined a graphene monolayer composite with functionalized platinum nanoparticles, which enhanced biomolecular immobilization. Graphene is an ideal transducer material due to its large surface area, high heterogeneous electron transfer rates, high intrinsic mobility and good electrical and thermal conductivity; the functionalized platinum nanoparticles have a large specific surface area, excellent biocompatibility, strong adsorption ability and good conductivity. In addition, Singal et al. [99] reported the good shelf-life stability of their immunosensor, as 96% of its initial sensitivity was retained (for 1.0 ng mL^{-1} of cTnI) after 30 days of

storage at 4°C. The optical immunosensor (based on fluorescence) was composed of a membrane strip installed within a cartridge to simultaneously detect cTnI and myoglobin, two biomarkers of acute myocardial infarction [100]. For cTnI, an LOD of 0.05 ng mL^{-1} was obtained with reproducible results (RSD of 7.5%) and a linear range of 0–50 ng mL^{-1}. Both cTnI biosensors can be used in clinical diagnostics considering a cut-off concentration of cTnI in the blood of 0.01–0.1 ng mL^{-1}. A concentration ranging between 0.1 and 2 ng mL^{-1} indicates unstable angina and other heart disorders, and a concentration greater than 2 ng mL^{-1} indicates significant myocardial injury and an increased risk of adverse cardiac events in future [99].

Myoglobin is used for early diagnosis of acute myocardial infarction. Its normal level in the blood (50–100 ng mL^{-1}) increases about 10–500 times in acute myocardial infarction [100]. With an optical immunosensor, Cho et al. [100] obtained reproducible results (RSD of 2.3%) and a linear range of 2.0–100 ng mL^{-1}. Four different potentially interfering substances (40 mg dL^{-1} bilirubin, 2000 mg dL^{-1} triglycerides, 2000 mg dL^{-1} haemoglobin and 100 mg dL^{-1} ascorbic acid) were also investigated for their effect on the immunoassay. Their presence did significantly alter (±5% variation) the result, compared with the negative control, except for the presence of bilirubin [100]. Zapp et al. [102] and Kim et al. [103] also recently developed immunosensors for myoglobin detection, as shown in Table 2, based on electrochemical and optical transduction principles, respectively. The electrochemical immunosensor offers a lower LOD (6.29 ng mL^{-1}) but a more narrow linear range (9.96–72.8 ng mL^{-1}) than those optical immunosensors (31.0 ng mL^{-1} and 100–1000 ng mL^{-1}, respectively). The immunosensor fabricated by Zapp et al. [102] is limited by the lack of validity in real samples; only simulated serum samples with myoglobin were used. Kim et al. [103] proposed an optical immunosensor based on SPR, which functions continuously in real time, reproducibly. They found acceptable variations in myoglobin levels over 8 hours with periodic one-point calibration every 3 hours (average CV of 4.91%), when tested in real serum samples. Thus, Kim et al. [103] recommended using the immunosensor along with real-time electrocardiographic measurement, for significantly more sensitive diagnosis of acute myocardial infarction diagnosis, thereby facilitating treatment at an early stage [103].

4.2. Sensors and biosensors for hormones, biomolecules and neurotransmitters

Table 4 includes the figures of merit for current sensors and biosensors (studies published between 2011 and 2015) to compare their analytical performance in detecting 1) hormones such as cortisol; 2) biomolecules such as glucose and cholesterol; and 3) neurotransmitters such as acetylcholine, epinephrine, norepinephrine and dopamine. Table 5 lists the normal values of these physiologically important analytes.

4.2.1. Hormones

Cortisol, a glucocorticoid hormone, is known to be a potential biomarker for estimating psychological stress. Abnormal cortisol levels are good indicators of chronic conditions such as Cushing's syndrome (symptoms of obesity, fatigue and bone fragility) at excess levels, or Addison's disease (manifested by weight loss, fatigue and darkening of skin folds and scars) at low levels [112,136]. The detection of cortisol is mostly limited to laboratory techniques such as chromatography, ELISA, SPR and QCM. These are limited by the long duration from sampling to results (from days to a few weeks), complex sample preparation and expensive diagnosis [111,112]. Thus, point-of-care technologies have been used to detect cortisol in relevant biological fluids such as saliva rapidly and selectively. The amount of free cortisol present in the saliva was significantly correlated with the total cortisol in the blood ($r = 0.60$; $p < 0.001$), with the normal levels of cortisol in serum ranging from 100 to 500 nM [131]. Recently, Pasha et al. [111] and Vabbina et al. [112] proposed electrochemical immunosensors based on cyclic voltammetry for the detection of cortisol in saliva samples (Table 4), the results of which were validated with ELISA methodology. Pasha et al. [111] constructed a simple, low-cost and label-free immunosensor based on interdigitated microelectrodes (IDEs), and Vabbina et al. [112] proposed a label-free, sensitive and selective immunosensor with nanomaterials (zinc oxide 1D nanorods and 2D nanoflakes) for the immobilization of cortisol antibodies. Both schematic representations of the immunosensing principle are shown in Fig. 4.

Pasha et al. [111] modified IDEs with a self-assembled monolayer (SAM) of dithiobis(succinimidylpropionate) for covalent immobilization of cortisol antibodies (anti-C_{ab}), as shown in Fig. 4i. Vabbina et al. [112] synthesized nanomaterials via a sonochemical technique, which were used to immobilize cortisol antibodies. Both immunosensors could detect cortisol in saliva samples. Furthermore, they can be used to monitor physiological stress for various conditions and to determine the physical, behavioural and psychological factors affecting the central nervous system.

Oestradiol or 17β-oestradiol, a natural steroid oestrogen, is also known to be endocrine disrupting, with an impact on reproductive and sexual functioning. Thus, quantifying their serum levels (normal levels are about 200–600 pg mL^{-1}) is crucial to various clinical evaluations for fertility treatments, postmenopausal status, hyperandrogenism and breast cancer [113,114]. Analytical techniques such as gas chromatography and high-performance liquid chromatography (HPLC) or electrochemical methods involving voltammetry and chronoamperometry have been used to determine oestradiol levels in biological, pharmaceutical and water samples. However, these techniques are labour and time intensive, requiring expensive equipment [113–115]. Thus, biosensors for oestradiol detection have been considered in the clinical field, due to their high selectivity and sensitivity. For example, Hao et al. [113] developed a sensor to detect oestradiol based on MWCNT and gold nanoparticles immobilized on a graphite electrode via a layer-by-layer assembling technique. The sensor was tested in serum samples from pregnant women using the standard addition method. The oestradiol content was determined, with good recoveries (98.5–103.5%) being reported, which indicates the applicability of this sensor in determining oestradiol in real samples. Ojeda et al. [114] proposed a disposable electrochemical immunosensor based on graphed *p*-aminobenzoic acid immobilized on screen-printed carbon electrodes to detect oestradiol. A low LOD (0.77 pg mL^{-1}) and a wide linear range (1.0–250 pg mL^{-1}) were obtained. The immunosensor was also used to analyse certified serum and spiked urine samples, with mean recoveries of 96–102% for serum samples and 95–100% for urine samples. Recently, Wang et al. [115] proposed an electrochemical sensor for oestradiol using nanoporous polymeric films on glass carbon electrodes, and good recoveries (99–103%) were reported when the sensor was applied to human urine samples, which demonstrates the applicability of the sensor to real samples. Wang et al. [115] also studied the selectivity of the sensor by measuring the current responses of some potential interfering substances such as L-cysteine, L-lysine and ascorbic acid (1.0×10^{-4} mol L^{-1}), as well as uric acid and tryptophan (5.0×10^{-5} mol L^{-1}). They found no interference (standard deviation lower than 5.0%) in the determination of 1.0×10^{-6} mol L^{-1} of oestradiol, which indicates good selectivity for oestradiol determination.

4.2.2. Biomolecules

The monitoring of glucose and cholesterol is crucial in the clinical diagnosis and treatment of diabetes mellitus and coronary heart diseases, respectively. The sensors recently proposed for their detection are listed in Table 4, which mainly used nanoparticles (CuO, Fe_2O_3 or ZnO) to enhance the analytical response. For example, Dung et al. [118], Yang et al. [119] and Zhang et al. [121]

Table 4
Analytical parameters of recently used clinical sensors and biosensors for hormones, biomolecules and neurotransmitters

Analyte detected (matrix)	Sensor type	Linear range	LOD[a]	Sensitivity (slope)	Additional information	References
HORMONES						
Cortisol (saliva samples)	Electrochemical immunosensor (interdigitated microelectrodes)	10–100,000 pg mL^{-1}	10 pg mL^{-1}	6 μA pg^{-1} mL^{-2}	r = 0.99	[111]
Cortisol (saliva samples)	Electrochemical immunosensor based on ZnO 1D nanorods and 2D nanoflakes	0.001–100 nM	0.001 nM	7.74–11.86 μA M^{-1}		[112]
Oestradiol (serum samples)	Electrochemical sensor based on MWCNT and Au nanoparticles (graphite electrodes)	70–42,000 nM	10 nM (S/N = 3)	7.57 μA $μM^{-1}$	RSD = 3.9%; n = 8 r = 0.994 Recovery = 98.5–103.5%	[113]
Oestradiol (serum and urine samples)	Electrochemical immunosensor based on graphed *p*-aminobenzoic acid (SPCE)	1.0–250 pg mL^{-1}	0.77 pg mL^{-1}		RSD = 5.9%; n = 8 r = 0.990 Recovery = 95–102%	[114]
Oestradiol (urine samples)	Electrochemical sensor based on nanoporous polymeric film (GCE)	100–10,000 nM	50 nM (S/N = 3)	0.1866 μA $μM^{-1}$	RSD = 4.3%; n = 5 r = 0.996 Recovery = 98.7–103.0%	[115]
BIOMOLECULES						
Glucose (serum samples)	Electrochemical immunosensor based on Ni nanoparticles and MWCNT	1–1000 μM	0.5 μM (S/N = 3)	1438 μA nM^{-1} cm^{-2}	r = 0.995 Recovery = 90.7–106.2%	[116]
Glucose (serum samples)	Electrochemical sensor based on graphene oxide and NiO nanofibres (GCE)		0.77 μM (S/N = 3)	1100 μA mM^{-1} cm^{-2}		[117]
Glucose (serum samples)	Electrochemical sensor based on CuO–SWCNT nanocomposites	0.05–1800 μM	0.050 μM	1610 μA mM^{-1} cm^{-2}		[118]
Glucose	Electrochemical enzymatic sensor based on carboxyl-modified graphene oxide and magnetic nanoparticles	100–1400 μM		1074.6 μA mM^{-1} cm^{-2}	RSD = 5.8% r^2 = 0.988	[119]
Glucose (serum samples)	Electrochemical sensor	2–15,000 μM	0.5 μM (S/N = 3)			[120]
Glucose	Electrochemical sensor based on CuO nanoparticles attached in carbon spheres (GCE)	0.5–2300 μM	0.1 μM (S/N = 3)	2981 μA mM^{-1} cm^{-2}	RSD = 1.6%; n = 6 r = 0.999 Recovery = 97.1–98.5%	[121]
Cholesterol (serum samples)	Optical enzymatic sensor based on CuO nanoparticles	0.625–12.5 μM	0.17 μM		RSD = 5.9%; n = 6 r = 0.9994 Recovery = 96.5–104.9%	[122]
Cholesterol (serum samples)	Electrochemical enzymatic biosensor based on Fe_2O_3 nanoparticles	100–8.0 mM	18 μM (S/N = 3)	78.56 μA mM^{-1} cm^{-2}	r^2 = 0.9951 Recovery = 95.0–98.0%	[123]
Cholesterol (serum samples)	Electrochemical enzymatic biosensor based on ZnO nanotubes	1.0–13,000 μM	0.0005 μM (S/N = 3)	79.40 μA mM^{-1} cm^{-2}	r = 0.9997	[124]
NEUROTRANSMITTERS						
Acetylcholine	Electrochemical enzymatic biosensor	0.001–1000 μM	0.00014 μM (S/N = 3)	7354 μA mM^{-1} cm^{-2}	RSD = 1.8% r = 0.9951	[125]
Acetylcholine	Electrochemical sensor based on MWCNT and ZnO nanoparticles	1.0–1000 μM	0.3 μM	180 μA mM^{-1} cm^{-2}		[126]
Choline (plasma samples)	Electrochemical sensor based on MWCNT and ZnO nanoparticles	1.0–800 μM	0.3 μM	178 μA mM^{-1} cm^{-2}	Recovery = 95–106%	[126]
Choline (serum samples)	Electrochemical enzymatic biosensor based on MWCNT and ZnO nanoparticles (GCE)	0.005–200 μM	0.01 μM	0.1929 mA $μM^{-1}$	CV = 2.97%; n = 6 r^2 = 0.9799	[127]
Epinephrine	Electrochemical biosensor based on fungal cells	5–100 μM	1.04 μM (3s/m)		CV = 3.83%; n = 5 r^2 = 0.9948	[128]
Epinephrine (urine samples)	Optical fibre sensor based on alginate/laccase matrix	8.2–205 ng L^{-1}	5.5 ng L^{-1} ($3y_0$+s)		r^2 = 0.9996	[129]
Epinephrine (urine samples)	Optical fibre sensor based on fluorescence	0.001–0.3 ng mL^{-1}	0.00088 ng mL^{-1} ($3y_0$+s)		r^2 = 0.9998 Recovery = 96–101%	[130]
Norepinephrine (urine samples)	Optical fibre sensor based on alginate/laccase matrix	8.9–222 ng L^{-1}	5.3 ng L^{-1} ($3y_0$+s)		r^2 = 0.9997	[129]
Norepinephrine (urine samples)	Optical fibre sensor based on fluorescence	0.001–0.3 ng mL^{-1}	0.00065 ng mL^{-1} ($3y_0$+s)		r^2 = 0.9998 Recovery = 96–101%	[130]
Dopamine (urine samples)	Optical fibre sensor based on alginate/laccase matrix	9.8–245 ng L^{-1}	4.1 ng L^{-1} ($3y_0$+s)		r^2 = 0.9996	[129]
Dopamine (urine samples)	Optical fibre sensor based on fluorescence	0.001–0.3 ng mL^{-1}	0.00059 ng mL^{-1} ($3y_0$+s)		r^2 = 0.9999 Recovery = 96–101%	[130]

CV: coefficient of variation; GCE: glassy carbon electrode; LOD: limit of detection; MWCNT: multiwalled carbon nanotubes; RSD: residual standard deviation; SPCE: screen-printed carbon electrode; SWCNT: single-walled carbon nanotubes.

[a] Determination of LOD: "S/N = 3": LOD is three times the signal-to-noise ratio; "3s/m": LOD is 3 times the standard deviation (s)/slope of calibration plot (m); "$3y_0$+s": LOD is 3 times the blank response (y_0) plus the standard deviation (s).

Table 5
Normal values of hormones, biomolecules and neurotransmitters in human blood

Analyte	Normal value	Reference
HORMONES		
Cortisol	100–500 nM	[131]
Oestradiol	200–600 pg mL^{-1}	[113]
BIOMOLECULES		
Glucose	4–8 mM	[132]
Cholesterol	5.2–6.2 mM	[133]
NEUROTRANSMITTERS		
Acetylcholine	1115–1413 pg mL^{-1}	[134]
Epinephrine	0.02–0.46 nM	[135]
Norepinephrine	0.45–2.49 nM	[135]
Dopamine	0.01–0.48 nM	[135]

used CuO–SWCNT nanocomposites, carboxyl-modified graphene oxide/magnetic nanoparticles and CuO nanoparticles/carbon spheres, respectively, for the detection of glucose with electrochemical sensors. Dung et al. [118] and Zhang et al. [121] reported the best sensitivities (2981 and 1610 μA mM^{-1} cm^{-2}, respectively) and wider linear ranges (0.05–1800 μM and 0.5–2300 μM, respectively) using non-enzymatic sensors, compared with the enzymatic-based sensor proposed by Yang et al. [119], with a sensitivity of 1074.6 μA mM^{-1} cm^{-2} and a linear range of 100–1400 μM (Table 4). Non-enzymatic sensors are preferred over sensors fabricated with enzymes, as the analytical applications of the former are limited by the high cost associated with enzyme isolation and purification and chemical and thermal deformation of enzymes. The non-enzymatic glucose sensors are based on direct oxidation of glucose at the electrode surface, with nanostructured metals (for example, Pt, Au, Ni or Cu) and metal oxides (for example, CuO or NiO) being used to enhance catalytic performance [116,121]. In addition, the analytical performance of such systems was also enhanced by the synergic interaction between various nanostructures used in the transduction mechanism . For example, Zhang et al. [121] reported the best sensitivity and wider linear range for the use of CuO nanoparticles attached to carbon spheres and immobilized on the glass carbon electrode, with no need for pre-surface modification. CuO nanoparticles have high specific surface area and good electrochemical activity, and they can promote electron transfer reactions at lower over-potential. Carbon spheres have an increasing electrochemical potential due to such physical properties as homogeneity of particle size, high specific surface area and conductivities [121]. The sensor was also highly selective for glucose in the presence of commonly interfering species such as ascorbic acid, dopamine, uric acid and chloride ion. It was successfully used to monitor the concentration of glucose in human serum samples [121].

Hong et al. [122], Umar et al. [123] and Ahmad et al. [124] used CuO nanoparticles, Fe_2O_3 nanoparticles and ZnO nanotubes, respectively, for sensors based on the transduction principle to detect cholesterol in serum samples. Ahmad et al. [124] obtained a lower LOD (0.0005 μM) for a high-performance cholesterol biosensor using ZnO grown on Si/Ag electrodes. The electrode displayed a response within 2 seconds with different concentrations of cholesterol (from 1.0 to 13,000 μM), as shown in Fig. 5i, which indicates the good catalytic property of the electrode [124]. In addition, the biosensor showed high stability for cholesterol detection, retaining about 93% of its original response to cholesterol after 60 days of storage. This stability can be attributed to the electron transfer between ZnO nanotubes and the electrode, the higher specific surface area of ZnO nanotubes and their ability to maintain the bioactivity of cholesterol oxidase, as stated by Ahmad et al. [124]. Based on the interference test, Ahmad et al. [124] found that the interfering species (glucose, ascorbic acid, L-cysteine and uric acid) did not affect the biosensor response visibly, which indicates that the fabricated biosensor is selective to cholesterol in the presence of various interfering species.

Umar et al. [123] proposed another electrochemical biosensor for cholesterol detection. Here, cholesterol oxidase was immobilized on Fe_2O_3 particles as the sensing active area, with a similar morphology to pine, as shown in Fig. 5iii. Such Fe_2O_3 micro-pine-shaped hierarchical structures were synthesized by a facile hydrothermal process at a large scale, and then characterized with

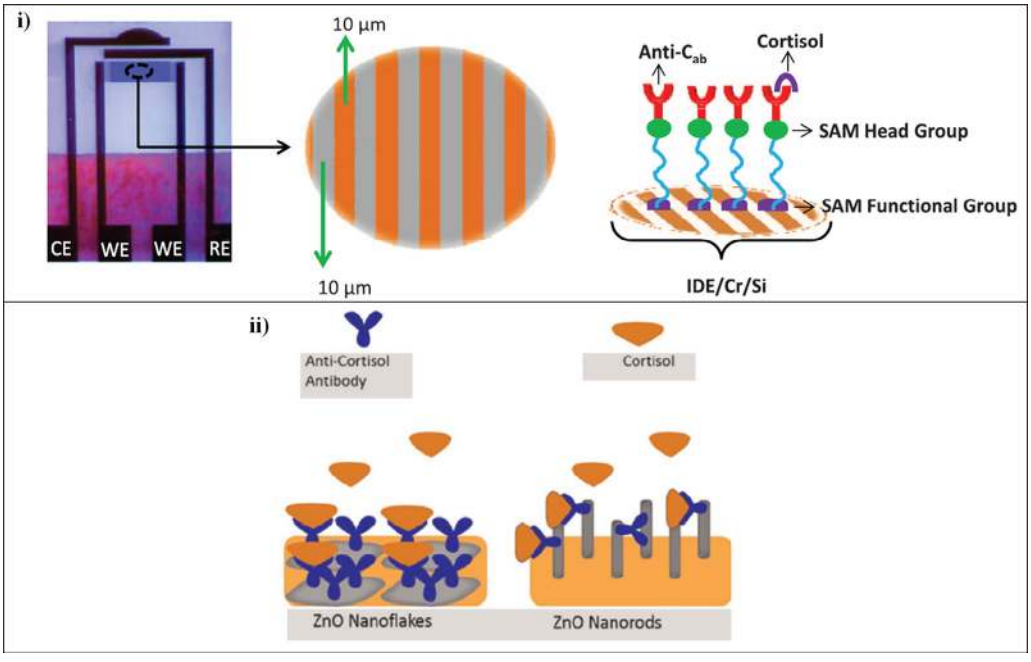

Fig. 4. i) Schematic representation of IDE, where the binding of cortisol with antibody (Anti-C_{ab}) blocks the electron transport from the medium to IDE and fabrication of immunosensor proposed by Pasha et al. [111] (Reproduced from Pasha et al. [111] by permission of The Electrochemical Society). CE: counter electrode; WE: working electrode; SAM: self-assembled monolayer; **ii)** Illustration of ZnO nanorods and ZnO nanoflakes along with immobilization of monoclonal anti-cortisol antibody to fabricate electrochemical cortisol immunosensor proposed by Vabbina et al. [112] (Reprinted from Vabbina et al. [112], with permission from Elsevier).

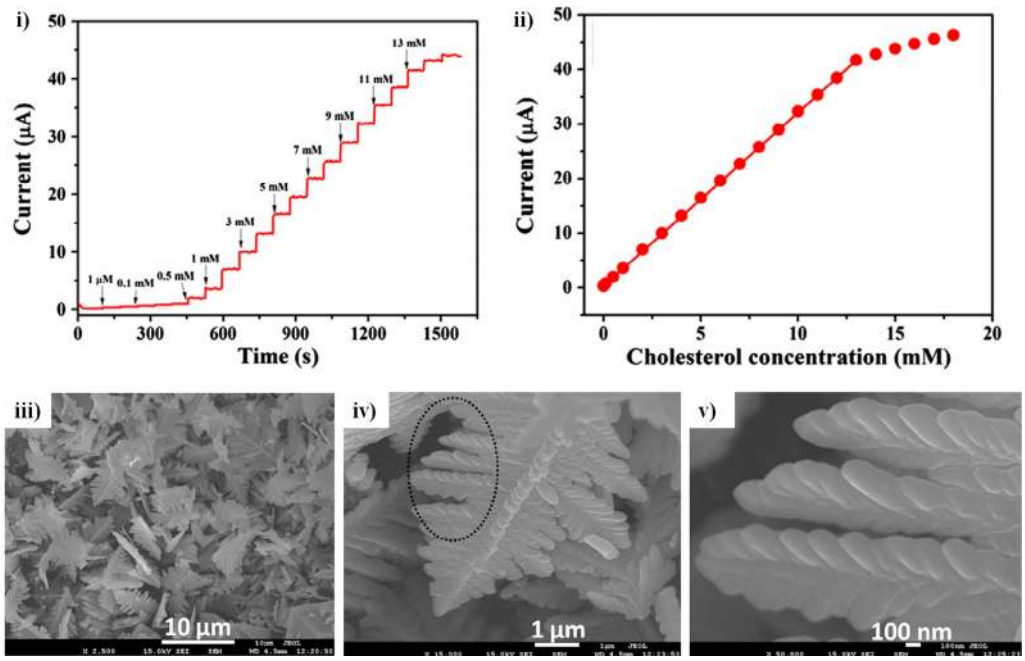

Fig. 5. **i)** Amperometric response to different cholesterol concentrations in 0.10 PBS at +0.38 V and **ii)** Calibration curve (Reprinted from Ahmad et al. [124], with permission from Elsevier). FESEM images of as-synthesized α-Fe_2O_3 micro-pine-shaped hierarchical structures at **iii)** low magnification, **iv)** and **v)** high resolution (Reprinted from Umar et al. [123], with permission from Elsevier).

field emission scanning electron microscopy (FESEM). Fig. 5iii shows an FESEM image illustrating the regular pine-shape morphology and very high density of Fe_2O_3 structures. Fig. 5iv and 5v demonstrate the highly crystalline and rhombohedral α-Fe_2O_3 crystal structures with a clear central trunk (~7 ± 2 μm), with highly ordered parallel branches (~3 ± 1 μm) being distributed on both sides of the trunk [109]. The authors attribute the high sensitivity (78.56 μA mM^{-1} cm^{-2}) to the large specific surface area of the micro-pine-shaped α-Fe_2O_3 hierarchical structures, enhanced cholesterol immobilization and direct and fast electron communication between the active sites and the electrode [123].

4.2.3. Neurotransmitters

Acetylcholine is a neurotransmitter present in both the peripheral and central nervous system of humans. Two sensors with different transduction principles are reported in Table 4. Rahman [125] fabricated an electrochemical sensor as a smart chip based on the enzymatic principle, with acetylcholine oxidase being immobilized on the electrode surface via peptide conjugation by amide bond formation. Conversely, Zhang et al. [126] developed an electrochemical sensor based on MWCNTs and ZnO nanoparticles for the detection of acetylcholine and choline, which is an enzymatic product of the oxidation of acetylcholine. Monitoring the levels of acetylcholine and choline is crucial for diagnosing neurodegenerative diseases such as Alzheimer's and neuromuscular diseases, myasthenia gravis and impaired cholinergic neurotransmission [127]. As shown in Table 4, the smart chip showed lower LOD and higher sensitivity, as the enzymes were immobilized onto the active sensitive surface via a simple and efficient approach, thus enhancing the sensor sensitivity to a large group of biomolecules. Thus, as stated by Rahman [125], the smart chip has a wide range of biomedical applications. In addition, the smart chip, fabricated by conventional photolithographic techniques, has other advantages such as its high sensitivity, small sample volume (70 μL), stability (1 month) and reproducibility (RSD of 1.8%). The main advantage of the electrochemical sensor proposed by Zhang et al. [126] is its long-term storage of 90 days. The unique multilayer structure (MWCNT–ZnO nanoparticles) provides a favourable microenvironment to maintain the bioactivity of choline oxidase and acetylcholinesterase. Zhang et al. [126] tested the sensor and an HPLC–mass spectrometry (MS)/MS technique for the detection of choline in human plasma samples. They obtained consistent analytical results: a mean concentration of total choline of 2.67 ± 0.21 mM in human plasma was obtained with the sensor and 2.54 ± 0.12 mM with the HPLC–MS/MS technique.

Epinephrine, also known as adrenaline, is one of the most important neurotransmitters in the central nervous system of mammals. It is present in the nervous tissue and body fluids in the form of large organic cations [128]. Determining the levels of neurotransmitters such as epinephrine, dopamine and norepinephrine in biological fluids is crucial for clinical analysis, as they are diagnostic biomarkers for a variety of metabolic and neurological disorders. For example, increased levels in urine have been used as a tumour marker for neuroblastoma and phaeochromocytoma, as well as increased stress [129]. Akyilmaz et al. [128] constructed a unique electrochemical biosensor based on fungal cells (from *Phanerochaete chrysosporium*) for the voltammetric determination of epinephrine (Table 4). In this biosensor, the fungal biomass was lyophilized and immobilized in gelatine on a platinum working electrode. Then, the immobilized cells were used as a source of laccase to develop the epinephrine biosensor; the current increases due to the redox activity of laccase in the biosensor, which released an epinephrinequinone [128]. According to the authors, the proposed biosensor has several advantages such as low cost and simplicity of construction compared with biosensors based on isolated enzymes. Other sensors for the detection of epinephrine as well as other neurotransmitters such as dopamine and norepinephrine in urine samples are listed in Table 4, which use optical fibres with an alginate/laccase matrix [129] or fluorescence [130]. The three neurotransmitters (dopamine, epinephrine and norepinephrine) were tested in the sensors constructed by Silva et al. [129] and Silva et al. [130]. A better LOD (0.00059–0.00088 ng mL^{-1}) was reported for the fluorescence sensor compared with the optical fibre sensor based on the alginate/laccase matrix, with an LOD of 4.1–5.5 ng mL^{-1}. When testing for dopamine, norepinephrine and epinephrine, figures of merit such as LOD (0.00059–0.00088 ng mL^{-1}) and the linear range (between

0.001 and 0.3 ng mL^{-1}) of the fluorescence optical fibre sensor were found to be superior to those of an HPLC–electrochemical detector (HPLC–ED) (0.0045–0.0051 ng mL^{-1} for the LOD and linear range between 0.005 and 0.125 ng mL^{-1}). Thus, Silva et al. [130] suggested the fluorescence sensor as a promising alternative to the current methodologies to determine catecholamines in clinical samples, due to its compact design, low-scale instrumentation and effective cost of analysis.

4.3. Sensors and biosensors for bacteria, virus and cancer cells

Table 6 includes the figures of merit of current sensors and biosensors (studies published between 2011 and 2015) to compare their analytical performance in the detection of 1) pathogenic bacteria such as *Escherichia coli*, 2) viruses such as hepatitis C virus core antigen and avian influenza virus and 3) cancer cells.

4.3.1. Bacteria

Traditional methods of detecting pathogenic bacteria such as *E. coli* and *Streptococcus pyogenes* involve cell culture and polymerase chain reaction (PCR). However, these methods are limited by the long processing times (24–48 hours of cultivation) or the need for high-cost equipment, preventing the rapid and *in situ* monitoring of such pathogens. Thus, these methods are not practical for point-of-care diagnostics. For example, Yang et al. [137] and Safavieh et al. [138] proposed two electrochemical immunosensors based on microfluidics for the detection of *E. coli* in urine samples (Table 6). Detection of *E. coli* in human urine is used to diagnose urinary tract infections commonly related to the kidney, as it is known to cause up to 80% of such infections and is present at concentrations $\geq 10^5$ CFU mL^{-1} [137]. Microfluidics reduces the consumption of costly reagents, as small volumes of liquid are manipulated in closed microscale channels. This increases the surface-to-volume ratio and

Table 6
Analytical parameters of recently used clinical sensors and biosensors for bacteria, virus and cancer cells

Analyte detected (matrix)	Sensor type	Linear range	LOD[a]	Sensitivity (slope)	Additional information	References
BACTERIA						
Escherichia coli (urine samples)	Electrochemical microfluidic immunosensor based on magnetic beads	6.4×10^4–6.4×10^8 CFU mL^{-1}	3.4×10^4 CFU mL^{-1} ($3y_0$+s)			[137]
E. coli (urine samples)	Electrochemical microfluidic immunosensor	4.8 -4.8×10^8 CFU mL^{-1}	24 CFU mL^{-1}			[138]
E. coli (serum samples)	Immunosensor based on epoxysilane (ITO)	10–10^6 CFU mL^{-1}	1 CFU mL^{-1}		RSD = 3%; n = 3 r^2 = 0.999	[139]
Streptococcus pyogenes (saliva samples)	Electrochemical immunosensor based on polytyramine (SPE)	10^4–10^7 cells mL^{-1}				[140]
VIRUS						
Hepatitis C virus core antigen	Electrochemical immunosensor based on Au nanoparticle–ZrO_2 nanoparticle–chitosan nanocomposite (GCE)	2–512 ng mL^{-1}	0.17 ng mL^{-1} (S/N = 3)	13.68 μA ng^{-1} mL^{-2}	RSD = 4.2%; n = 5 r = 0.9968	[141]
Hepatitis C virus core antigen (serum samples)	Electrochemical immunosensor based on mesoporous carbon–methylene blue nanocomposites	0.00025–0.3 ng mL^{-1}	0.00001 ng mL^{-1} (S/N = 3)	355 μA pg^{-1} mL^{-2}	RSD = 5.2%; n = 5 r = 0.997 Recovery = 94.8–105.6%	[142]
Avian influenza virus H1N1	Electrochemical immunosensor based on SWCNT	1–10^4 PFU mL^{-1}	1 PFU mL^{-1}		r^2 = 0.99	[143]
Avian influenza virus H9N2	Electrochemical immunosensor based on magnetic beads	50–2000 ng mL^{-1}	1 ng mL^{-1} (S/N = 3)		RSD = 4.8%; n = 3 r = 0.997	[144]
Dengue virus NS1 protein (serum samples)	Electrochemical immunosensor based on carboxylated MWCNT (SPE)	40 ng mL^{-1}–2 μg mL^{-1}	12 ng mL^{-1}	85.59 μA mM^{-1} cm^{-2}	CV = 3.4%; n = 6 r = 0.996 Recovery = 98–116%	[145]
CANCER CELLS						
Leukaemia cells	Electrochemical cytosensor based on HRP and gold nanoparticle-decorated magnetic Fe_3O_4 beads	10^3–10^6 cells mL^{-1}	660 cells mL^{-1}		r = 0.995	[146]
Human cervical carcinoma cells	Electrochemical cytosensor based on ferrocene and SWCNT	10–10^6 cells mL^{-1}	10 cells mL^{-1}		RSD = 2.8%; n = 5	[147]
Human non-small-cell lung cancer cells	Electrochemical cytosensor based on hydrazine and aptamers attached to gold nanoparticles	15–10^6 cells mL^{-1}	8 cells mL^{-1}		RSD = 2.8%; n = 10 r = 0.9987	[148]
Human liver cancer cells	Electrochemical cytosensor based on aptamers, horseradish peroxidase and gold nanoparticles	10^2–10^7 cells mL^{-1}	30 cells mL^{-1}		RSD = 3.7%; n = 3 r = 0.9952	[149]
Human liver cancer cells	Electrochemical cytosensor based on aptamers and gold nanoparticles	10^2–10^7 cells mL^{-1}	15 cells mL^{-1}		RSD = 5.6%; n = 3 r = 0.9917	[150]

CFU: colony-forming unit; CV: coefficient of variation; GCE: glassy carbon electrode; HRP: horseradish peroxidase; ITO: indium tin oxide electrode; LOD: limit of detection; MWCNT: multiwalled carbon nanotubes; PFU: plaque-forming unit; RSD: residual standard deviation; SPE: screen-printed electrode; SWCNT: single-walled carbon nanotubes.
[a] Determination of LOD: "S/N = 3": LOD is three times the signal-to-noise ratio; "$3y_0$+s": LOD is 3 times the blank response (y_0) plus the standard deviation (s).

enhances the ongoing reactions, thus leading to miniaturized biosensors with various applications [138]. The biosensor fabricated by Yang et al. [137] is considered as a lab on a chip, consisting of two chambers (for concentration and sensing) connected in series and an integrated impedance detector. These two chambers help reduce the non-specific absorption of proteins such as albumin, which coexists with *E. coli* in urine, thereby improving the sensitivity. In the concentration chamber, the bacteria are separated from the urine sample by the conjugation of microsized magnetic beads to *E. coli* antibodies. The immobilized *E. coli* is then transferred to the sensing chamber to measure impedance and in turn estimate the *E. coli* concentration [137]. With this portable biosensor, an LOD of 3.4×10^4 CFU mL^{-1} was obtained, which is lower that the threshold of urinary tract infections (10^5 CFU mL^{-1}). The LOD obtained with the microfluidic biosensor proposed by Safavieh et al. [138] was greater (24 CFU mL^{-1}) than that obtained by Yang et al. [137]. Safavieh et al. [138] developed a biosensor employing loop-mediated isothermal amplification, which played a key role in quantifying the bacteria. Isothermal amplification techniques can amplify the target nucleic acids at constant temperature. For example, loop-mediated isothermal amplification is accurate, rapid and cost-effective with high sensitivity and specificity, amplifying a few copies of DNA to 10^9 copies in less than an hour at 60–66°C [138]. Recently, Barreiros dos Santos et al. [139] reported the construction of a label-free immunosensor based on epoxysilane, with an LOD of 1 CFU mL^{-1}, lower than those reported previously. The biosensor was composed of ITO electrodes, with the antibodies specific to *E. coli* being immobilized via covalent attachment to epoxysilane. The authors attributed the low LOD to the robust surface functionalization, which was based on the immobilization of biomolecules via silane monolayers using trifunctional silanes. The immunosensor also showed good reproducibility (RSD of 3%) and good stability (48 hours at 4°C). Barreiros dos Santos et al. [139] also tested a traditional technique (ELISA) for the detection of *E. coli* in urine samples in order to compare the analytical results. However, they obtained a higher LOD (10^4 CFU mL^{-1}). The same research group [151] previously developed another immunosensor for the detection of *E. coli* but using gold substrates rather than ITO electrodes. They showed that despite the similar LODs (2 CFU mL^{-1}), the ITO required lesser experimental time. Moreover, the immobilization of antibodies onto ITO required 4 hours, whereas functionalization of the gold electrode was an overnight process.

4.3.2. Virus

The most sensitive and specific assays for detecting infectious diseases are PCR and ELISA. However, they are unsuited for clinical screening or point-of-care diagnostics as they are time and cost intensive. Thus, immunosensors have been considered as an alternate diagnostic tool as they are simple, fast, label-free and of low cost [152].

Hepatitis C virus causes chronic viral hepatitis, which can develop into cirrhosis and hepatocellular carcinoma. Thus, early detection is crucial for preventing chronic infection [141]. Avian influenza virus is spread easily via air, with infection acquired through the respiratory system. Thus, rapid, reliable methods of detecting the influenza virus are needed, as conventional virus detection methods such as diagnostic test kits, ELISA and PCR are poor in specificity, low in sensitivity, time consuming and expensive, and they require a laboratory and a trained technician [143]. Recently used immunosensors are listed in Table 6 for the detection of hepatitis C virus core antigen, avian influenza virus and dengue virus, all of which used nanomaterials. For example, Ma et al. [141] used gold nanoparticles and zirconia nanoparticles (inorganic oxide with thermal stability and chemical inertness without toxicity) in a chitosan nanocomposite to construct an immunosensor based on glass carbon electrodes to detect hepatitis C virus core antigen. Singh et al. [143] used SWCNTs to develop an immunosensor to detect the avian influenza virus. Both schematic representations of the construction of immunosensors and SEM images of nanomaterials immobilized in sensing platforms are shown in Fig. 6.

The label-free amperometric immunosensor reported by Ma et al. [141] showed high sensitivity to the hepatitis C virus core antigen (13.7 μA ng^{-1} mL^{-2}) in the concentration range 2–512 ng mL^{-1}, with an LOD of 0.17 ng mL^{-1}. The SEM image in Fig. 6ii(a) displays zirconia-chitosan nanoparticles with smooth morphology and a diameter of about 100 nm, as indicated by the solid arrow. The SEM image in Fig. 6ii(b) displays the morphologies of nanocomposites with immobilized hepatitis C virus core antibodies, which were greater in size than zirconia nanoparticles alone (Fig. 6ii(a)). In addition, the immunosensor exhibited high reproducibility (RSD of 4.2%) and high stability, as the immunosensor could retain about 98.5% of the initial current response after a storage period of 30 days at 4°C, due to the good biocompatibility of gold–zirconia–chitosan nanocomposites with the immobilized antibodies [141]. The immunosensor was tested in six serum samples, the results of which were compared to those of a traditional ELISA technique. The concentrations of hepatitis C virus core antigen were similar, with relative deviations of the proposed immunosensor in the range of –4.35% to 6.65%. Thus, this immunosensor can be an alternative tool for the clinical detection of hepatitis C virus core antigen in human serum samples. For the detection of avian influenza virus, the SWCNT immunosensor reported by Singh et al. [143] displays an LOD of 1 PFU mL^{-1} in a linear concentration range of 1–10^4 PFU mL^{-1} with a detection time of 30 minutes. In Fig. 6iv(a) and 6iv(b), uniformly distributed, aligned and aggregation-free SWCNTs are observed after the PDDA assembly. The majority of the individual SWCNTs were reasonably aligned parallel to the electrodes, and the deposited SWCNTs were reproducible due to the PDDA monolayer (Fig. 6iv(c)). Furthermore, avidin and biotinylated antibodies were successfully immobilized onto the SWCNT surfaces, as reflected by the uniform morphology in Fig. 6iv(d). Fig. 6iv(e) displays a single influenza virus captured by the antibodies distributed on the SWCNTs with several virus aggregates [143]. According to the authors, the immunosensors can form an important component of a point-of-care test kit for rapid and simple clinical diagnosis or a component of a portable lab-on-a-chip system.

Dengue is a self-limiting, non-specific illness characterized by fever, headache, myalgia and constitutional symptoms. In its severe forms (haemorrhagic fever and shock syndrome), it may progress to multisystem involvement and death, mostly in children [145]. Kumbhat et al. [153] called for a timely diagnosis of dengue virus in vectors and humans with real-time biosensors to prevent its spread, in addition to the current gold-standard serological tests such as ELISA and immunofluorescence assays to detect specific antibody and viral antigen Dias et al. [145] proposed an amperometric immunosensor for the detection of the non-structural protein 1 (NS1) of the dengue virus, using carboxylated MWCNTs on screen-printed electrodes with antibodies being covalently linked to this transducing platform (Table 6). In primary infections, the NS1 levels range from 0.04 to 2 μg mL^{-1} in serum samples of patients in the acute disease phase (up to 7 days) [145]. According to the authors, the proposed imunosensor is a point-of-care approach that diagnoses the early clinical phase of dengue infection. This conclusion was based on successful analytical results with spiked blood serum samples, considered the excellent recovery values (98–116%), excellent LOD (12 ng mL^{-1}) and sensitivity of 85.59 μA mM^{-1} cm^{-2} [145].

4.3.3. Cancer cells

Cytosensors have been recently developed for the detection of cancer cells, as they require simple instrumentation and reduce the cost and time required for analysis [147]. For example, Zheng et al. [146] developed a robust electrochemical cytosensing approach for both the selective detection of leukaemia cells with LODs as low as ~40 cells and the quantitative evaluation of the DR4/DR5 expression

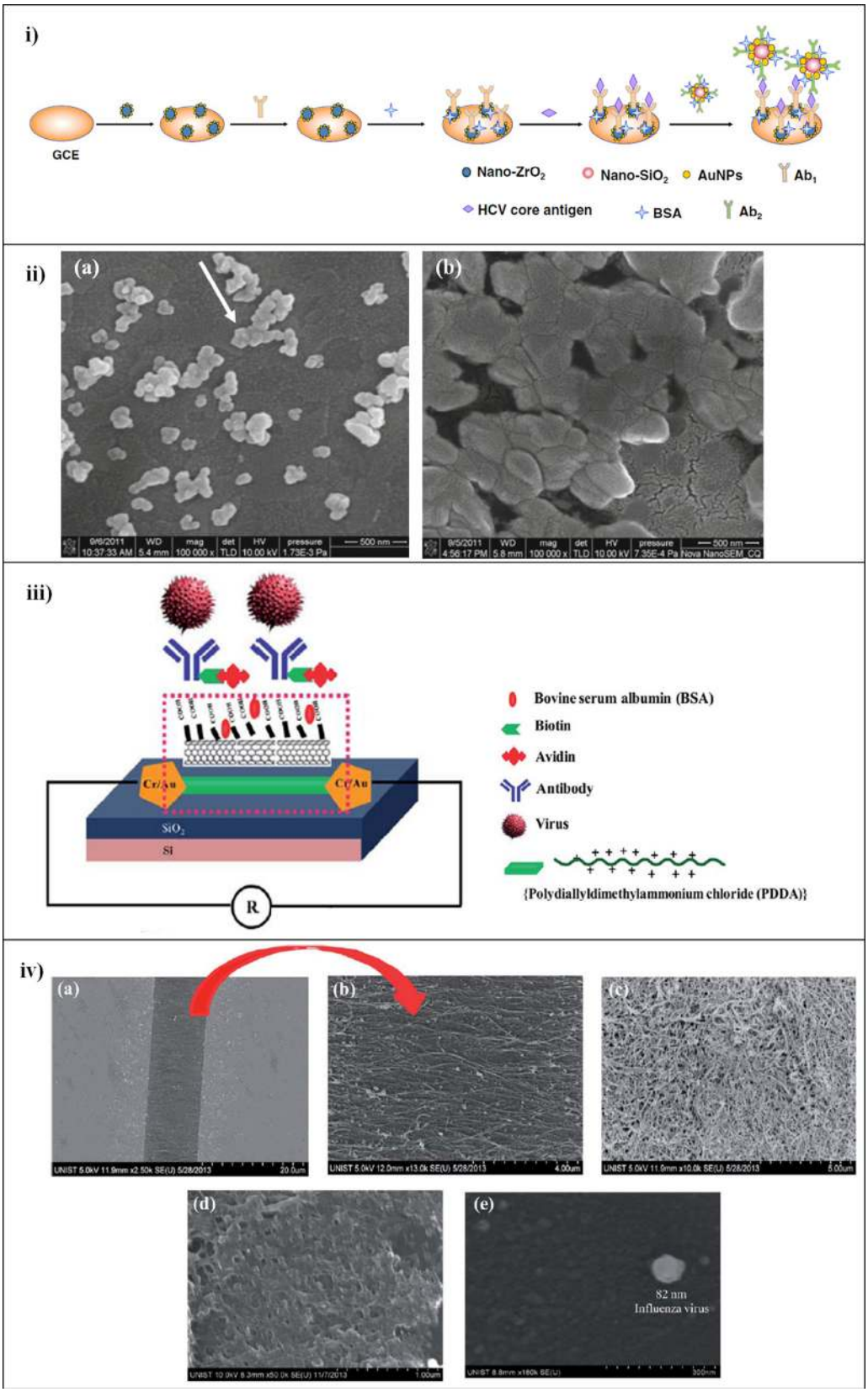

Fig. 6. **i)** Fabrication and measurement procedures for the immunosensor proposed by Ma et al. [141] and **ii)** Sizes and morphologies of nanocomposites [(a) SEM images of ZrO_2 nanoparticle–chitosan and (b) antibody–Au nanoparticle–ZrO_2 nanoparticle–chitosan] (With kind permission from Springer Science+Business Media: Microchimica Acta, Ma et al. [141]); **iii)** Schematic illustration of the SWCNT immunosensor for H1N1 virus detection proposed by Singh et al. [143] and **iv)** SEM images of (a) PDDA–SWCNT, (b) PDDA–SWCNT at higher magnification, (c) SWCNT deposited by sedimentation, (d) H1N1 antibody immobilized on PDDA–SWCNT and (e) H1N1 antibody immobilized on PDDA–SWCNT after capturing a single influenza virus (Reproduced from Singh et al. [143] by permission of The Royal Society of Chemistry).

status on leukaemia cell surfaces. The expression of DR4 and DR5, which are death receptors, can be quantified on leukaemia cell surfaces as important diagnostic tools to guide death receptor-based leukaemia treatment [146]. Electrochemical cytosensors can comprise the following: a) multifunctional hybrid nanoprobes used for cytosensing, which are based on horseradish peroxidase and Au nanoparticle-decorated magnetic Fe_3O_4 beads, for the specific recognition of DR4/DR5 on leukaemia cell surfaces, and b) nano-architectured electrode interfaces, which specifically target the analytes and facilitate significant electron transfer between the analytes and electrodes [146]. According to the authors, the multifunctional hybrid nanoprobes and the nano-architectured electrode interface amplify the signal, in turn lowering the LOD. In addition, the electrochemical cytosensing platform is considered to be of great clinical value for the early diagnosis of human leukaemia and the evaluation of the effects of radiation or drug therapy on leukaemia patients [146]. Liu et al. [147] constructed a label-free electrochemical cytosensor with surface-confined ferrocene as the signal indicator and SWCNTs for the selective detection of human cervical carcinoma cells. This cytosensor has a wide detection range ranging from 10 to 10^6 cells mL^{-1} with an LOD as low as 10 cells mL^{-1}, which was reached even in the presence of a large amount of non-cancerous cells. The poly(ethylyimine) functionalized with ferrocene was used as the signal indicator and assembled on the electrode surface, thus providing an amplified signal to improve the detection sensitivity [147]. Recently, Mir et al. [148] constructed a nanobiosensor for the selective detection of human non-small-cell lung cancer cells using hydrazine and aptamers attached on gold nanoparticles to amplify the signal. Sensitive and accurate early diagnosis of lung cancer is necessary for its prevention, assessment of therapeutic efficacy and detection of minimal residual disease. This is because if the associated cancerous cells are recognized in the early stages of lung cancer, the treatment and five-year survival rates exceed 60% [148]. In the cytosensor proposed by Mir et al. [148], the lung cancer cells were recognized by the strong interaction between their glycoproteins on the cell membrane surface and specific aptamers, with an excellent dynamic range from 15 to 1×10^6 cells mL^{-1} and an LOD of 8 cells mL^{-1}. According to the authors, the proposed cytosensor is a simple, low-cost and biocompatible strategy for the sensitive analysis of non-small-cell lung cancer, which can also be used to differentiate between cancerous and non-cancerous cells, and to facilitate early clinical diagnosis and treatment of non-small-cell lung cancer and related diseases. The same research group detected human liver hepatocellular carcinoma cells using cytosensors but with two types of sensing principles. Sun et al. [149] proposed an electrochemical cytosensor based on aptamers covalently attached to a gold electrode to capture the cancerous cells using horseradish peroxidase and gold nanoparticles in the sensing probe. Alternatively, Sun et al. [150] proposed an electrochemical cytosensor based on aptamers but attached on a glassy carbon electrode with gold nanoparticles. Both electrochemical cytosensors provided a wide detection range from 10^2 to 10^7 cells mL^{-1} but with different LODs, 30 cells mL^{-1} obtained by Sun et al. [149] and 15 cells mL^{-1} by Sun et al. [150]. The advantage of such cytosensors is the regeneration of the sensing system through an electrochemical reductive desorption method, which breaks the gold–thiol bond and removes all components on the gold nanoparticle/glassy carbon electrode surface. For example, Sun et al. [150] reported that the regenerating cytosensor retained 90% of its original sensitivity twice for cancer cell detection.

5. Conclusions and future prospects

This review covered the recent clinical applications of sensors and biosensors for the detection and monitoring of different physiologically important analytes such as cancer and cardiac biomarkers, hormones, biomolecules, neurotransmitters, bacteria, virus and cancer cells. The analytical performance of these sensors and biosensors was compared. Electrochemical biosensors are most widely used, due to their miniaturization, easy handling and portability. They are also promising point-of-care tools, due to their high sensitivity and selectivity, rapid response and low cost. At present, the fabricated sensors and biosensors are being increasingly used to detect physiologically important analytes in real biological samples (blood serum and plasma, urine and saliva), as shown in Tables 2, 4 and 6, compared with the literature and our previous paper [3]. Recently, saliva has been considered an alternative sample for the determination of various analytes such as IL-6, CRP and cortisol with biosensors. Saliva collection is non-invasive, cost-effective, pain-free and stress-free, and it does not require special laboratory equipment [154]. Furthermore, advances have been made in the development of nanoscale and microscale biosensors for point-of-care testing of salivary analytes. Prototypes of sensors and biosensors in the clinical field are mainly developed for glucose and cholesterol detection. They are then used as point-of-care devices for routine diagnosis. Further concerns in the clinical application of current sensors and biosensors include enhancing their stability for other physiologically important analytes such as cancer and cardiac biomarkers, as well as hormones or neurotransmitters. The concentrations of these analytes are influenced by interfering molecules in real biological samples. This is particularly important for determining the analytical performance of an analytical technique, as reflected in the guidelines of the Clinical and Laboratory Standards Institute [155]. These guidelines offer background information, guidance and experimental procedures for investigating, identifying and characterizing the effects of interfering substances on the test results. With respect to sensors and biosensors, recent studies have reported using specific recognition elements (such as synthesized elements as aptamers) to determine physiologically important analytes and facilitate chemical surface modification of solutions. This reduces the non-specific binding of interfering molecules, in turn enhancing the sensor selectivity [12]. In addition, the analytical performance of sensors and biosensors is enhanced by increasing their figures of merit, which is a major development in analytical chemistry. Further, this should be considered when developing commercial sensing systems from prototypes. All figures of merit should be considered in the validation of sensors and biosensors, for both clinical and practical applications such as food safety and environmental monitoring. Studies verifying the selectivity of sensors and biosensors are lacking. Testing the selectivity is crucial to ascertain whether the method can accurately quantify an analyte in the presence of interferences [3].

Acknowledgements

This work was funded by the Portuguese Science Foundation (FCT) through scholarships (ref. SFRH/BPD/95961/2013) under POCH funds, co-financed by the European Social Fund and Portuguese National Funds from MEC. This work was also funded by national funds via FCT/MEC (PIDDAC) under project IF/00407/2013/CP1162/CT0023. The authors acknowledge the financial support to CESAM (UID/AMB/50017), to FCT/MEC through national funds and the co-funding by the FEDER, within the PT2020 Partnership Agreement and Compete 2020.

References

[1] C.I.L. Justino, T.A.P. Rocha-Santos, A.C. Duarte, Advances in point-of-care technologies with biosensors based on carbon nanotubes, Trends Anal. Chem. 45 (2013) 24–36.
[2] B. Giri, B. Pandey, B. Neupane, F.S. Ligler, Signal amplification strategies for microfluidic immunoassays, Trends Anal. Chem. 79 (2015) 326–334.

[3] C.I.L. Justino, T.A.P. Rocha-Santos, A.C. Duarte, Review of analytical figures of merit of sensors and biosensors in clinical applications, Trends Anal. Chem. 29 (2010) 1172–1183.
[4] C.I.L. Justino, A.C. Duarte, T.A.P. Rocha-Santos, Immunosensors in clinical laboratory diagnostics, Adv. Clin. Chem. 73 (2016) 65–108.
[5] D.R. Thévenot, K. Toth, R.A. Durst, G.S. Wilson, Electrochemical biosensors: recommended definitions and classification, Biosens. Bioelectron. 16 (2001) 121–131.
[6] M. Farré, L. Kantiani, S. Pérez, D. Barceló, Sensors and biosensors in support of EU Directives, Trends Anal. Chem. 28 (2009) 170–185.
[7] M. Hasanzadeh, N. Shadjou, M. Eskandani, M. de la Guardia, E. Omidinia, Electrochemical nano-immunosensing of effective cardiac biomarkers for acute myocardial infarction, Trends Anal. Chem. 49 (2013) 20–30.
[8] M. Pedrero, S. Campuzano, J.M. Pingarrón, Electrochemical biosensors for the determination of cardiovascular markers: a review, Electroanalysis 26 (2014) 1132–1153.
[9] N.J. Ronkainen, S.L. Okon, Nanomaterial-based electrochemical immunosensors for clinically significant biomarkers, Materials 7 (2014) 4669–4709.
[10] E.B. Bahadir, M.K. Sezgintürk, Applications of electrochemical immunosensors for early clinical diagnosis, Talanta 132 (2015) 162–174.
[11] S. Vaddiraju, I. Tomazos, D.J. Burgess, F.C. Jain, F. Papadimitrakopoulos, Emerging synergy between nanotechnology and implantable biosensors: a review, Biosens. Bioelectron. 25 (2010) 1553–1565.
[12] C.I.L. Justino, A.C. Freitas, R. Pereira, A.C. Duarte, T.A.P. Rocha-Santos, Recent developments in recognition elements for chemical sensors and biosensors, Trends Anal. Chem. 68 (2015) 2–17.
[13] C.I.L. Justino, T.A.P. Rocha-Santos, S. Cardoso, A.C. Duarte, Strategies for enhancing the analytical performance of nanomaterial-based sensors, Trends Anal. Chem. 47 (2013) 27–36.
[14] C. Fenzl, T. Hirsch, A.J. Baeumner, Nanomaterials as versatile tools for signal amplification in (bio)analytical applications, Trends Anal. Chem. 79 (2015) 306–316.
[15] M. Hasanzadeh, N. Shadjou, Electrochemical nanobiosensing in unprocessed whole blood: recent advances, Trends Anal. Chem. 80 (2016) 167–176.
[16] A.P.F. Turner, Biosensors: sense and sensibility, Chem. Soc. Rev. 42 (2013) 3184–3196.
[17] A.C. Olivieri, N.M. Faber, J. Ferré, R. Boqué, J.H. Kalvas, H. Mark, Uncertainty estimation and figures of merit for multivariate calibration (IUPAC Technical Report), Pure Appl. Chem. 78 (2006) 633–661.
[18] P. D'Orazio, Biosensors in clinical chemistry – 2011 update, Clin. Chim. Acta 412 (2011) 1749–1761.
[19] H. Ju, X. Zhang, J. Wang, Nanobiosensing for clinical diagnosis, in: H. Ju, X. Zhang, J. Wang (Editors), NanoBiosensing: Principles, Development and Application, Springer, Berlin, 2011, pp. 535–567.
[20] J. Zhang, S.P. Song, L.Y. Zhang, L.H. Wang, H.P. Wu, D. Pan, et al., Sequence specific detection of femtomolar DNA via a chronocoulometric DNA sensor (CDS): effects of nanoparticle-mediated amplification and nanoscale control of DNA assembly at electrodes, J. Am. Chem. Soc. 128 (2006) 8575–8580.
[21] H. Zhang, L. Liu, X. Fu, Z. Zhu, Microfluidic beads-based immunosensor for sensitive detection of cancer biomarker proteins using multienzyme-nanoparticle amplification and quantum dots labels, Biosens. Bioelectron. 42 (2013) 23–30.
[22] S.H. Baek, A.W. Wark, H.J. Lee, Dual nanoparticle amplified Surface Plasmon Resonance detection of thrombin at subattomolar concentrations, Anal. Chem. 86 (2014) 9824–9829.
[23] Y. Feng, T. Yang, W. Zhang, C. Jiang, K. Jiao, Enhanced sensitivity for deoxyribonucleic acid electrochemical impedance sensor: gold nanoparticle/polyaniline nanotube membranes, Anal. Chim. Acta 616 (2008) 144–151.
[24] L. Wang, J. Wang, S. Zhang, Y. Sun, X. Zhu, Y. Cao, et al., Surface plasmon resonance biosensor based on water-soluble ZnO-Au nanocomposites, Anal. Chim. Acta 653 (2009) 109–115.
[25] Q. Wang, J. Zheng, Electrodeposition of silver nanoparticles on a zinc oxide film: improvement of amperometric sensing sensitivity and stability for hydrogen peroxide determination, Microchim. Acta 169 (2010) 361–365.
[26] M.L. Lozano, M.C. Rodriguez, P. Herrasti, L. Galicia, G.A. Rivas, Amperometric response of hydrogen peroxide at carbon nanotube paste electrodes modified with an electrogenerated poly(Fe(III)-5-amino-phenantroline). Analytical applications for glucose biosensing, Electroanalysis 22 (2010) 128–134.
[27] L. Guo, Y. Xu, A.R. Ferhan, G. Chen, D.-H. Kim, Oriented gold nanoparticle aggregation for colorimetric sensors with surprisingly high analytical figures of merit, J. Am. Chem. Soc. 135 (2013) 12338–12345.
[28] X. Sun, L. Qiao, X. Wang, A novel immunosensor based on Au nanoparticles and polyaniline/multiwall carbon nanotubes/chitosan nanocomposite film functionalized interface, Nano-Micro Lett. 5 (2013) 191–201.
[29] F. Wei, P.B. Lillehoj, C.M. Ho, DNA diagnostics: nanotechnology-enhanced electrochemical detection of nucleic acids, Pediatr. Res. 67 (2010) 458–468.
[30] B. Kavosi, R. Hallaj, H. Teymourian, A. Salimi, Au nanoparticles/PAMAM dendrimer functionalized wired ethyleneamine–viologen as highly eficiente interface for ultrasensitive a-fetoprotein electrochemical immunosensor, Biosens. Bioelectron. 59 (2014) 389–396.
[31] H. Zhou, N. Gan, T. Li, Y. Cao, S. Zeng, L. Zheng, et al., The sandwich-type electrochemiluminescence immunosensor for a-fetoprotein based on enrichment by Fe_3O_4–Au magnetic nano probes and signal amplification by CdS–Au composite nanoparticles labeled anti-AFP, Anal. Chim. Acta 746 (2012) 107–113.
[32] L. Xie, L. You, X. Cao, Signal amplification aptamer biosensor for thrombin based on a glassy carbon electrode modified with graphene, quantum dots and gold nanoparticles, Spectrochim. Acta A. Mol. Biomol. Spectrosc. 109 (2013) 110–115.
[33] D. Du, Z. Zou, Y. Shin, J. Wang, H. Wu, M.H. Engelhard, et al., Anal. Chem. 82 (2010) 2989–2995.
[34] D. Fu, H. Okimoto, C.W. Lee, T. Takenobu, Y. Iwasa, H. Kataura, et al., Ultrasensitive detection of DNA molecules with high ON/OFF single-walled carbon nanotube network, Adv. Mater. 22 (2010) 4867–4871.
[35] F.N. Ishikawa, M. Curreli, C.A. Olson, H.-I. Liao, R. Sun, R.W. Roberts, et al., Importance of controlling nanotube density for highly sensitive and reliable biosensors functional in physiological conditions, ACS Nano 4 (2010) 6914–6922.
[36] S. Okuda, S. Okamoto, Y. Ohno, K. Maehashi, K. Inoue, K. Matsumoto, Horizontally aligned carbon nanotubes on a quartz substrate for chemical and biological sensing, J. Phys. Chem. C 116 (2012) 19490–19495.
[37] M. Lee, J. Lee, T.H. Kim, H. Lee, B.Y. Lee, J. Park, et al., 100 nm scale low-noise sensors based on aligned carbon nanotube networks: overcoming the fundamental limitation of network-based sensors, Nanotechnology 21 (2010) 055504.
[38] J. Li, Y. Zhang, S. To, L. You, Y. Sun, Effect of nanowire number, diameter, and doping density on nano-FET biosensor sensitivity, ACS Nano 5 (2011) 6661–6669.
[39] N. Granqvist, A. Hanning, L. Eng, J. Tuppurainen, T. Viitala, Label-enhanced surface plasmon resonance: a new concept for improved performance in optical biosensor analysis, Sensors (Basel) 13 (2013) 15348–15363.
[40] W. Shen, D. Tian, H. Cui, D. Yang, Z. Bian, Nanoparticle-based electrochemiluminescence immunosensor with enhanced sensitivity for cardiac troponin I using N-(aminobutyl)-N-(ethylisoluminol)-functionalized gold nanoparticles as labels, Biosens. Bioelectron. 27 (2011) 18–24.
[41] B. Su, D. Tang, Q. Li, J. Tang, G. Chen, Gold–silver–graphene hybrid nanosheets-based sensors for sensitive amperometric immunoassay of alpha-fetoprotein using nanogold-enclosed titania nanoparticles as labels, Anal. Chim. Acta 692 (2011) 116–124.
[42] M. Zhang, S. Ge, W. Li, M. Yan, X. Song, J. Yu, et al., Ultrasensitive electrochemiluminescence immunoassay for tumor marker detection using functionalized Ru-silica@nanoporous gold composite as labels, Analyst 137 (2012) 680–685.
[43] T.A.P. Rocha-Santos, Sensors and biosensors based on magnetic nanoparticles, Trends Anal. Chem. 62 (2014) 28–36.
[44] Y. Wang, J. Dostalek, W. Knoll, Magnetic nanoparticle-enhanced biosensor based on grating-coupled Surface Plasmon Resonance, Anal. Chem. 83 (2011) 6202–6207.
[45] F. Liu, Y. Zhang, S. Ge, J. Lu, J. Yu, X. Song, et al., Magnetic graphene nanosheets based electrochemiluminescence immunoassay of cancer biomarker using CdTe quantum dots coated silica nanospheres as labels, Talanta 99 (2012) 512–519.
[46] C. Yao, T. Zhu, Y. Qi, Y. Zhao, H. Xia, W. Fu, Development of a quartz crystal microbalance biosensor with aptamers as bio-recognition element, Sensors (Basel) 10 (2010) 5859–5871.
[47] D. Du, L. Wang, Y. Shao, J. Wang, M.H. Engelhard, Y. Lin, Functionalized graphene oxide as a nanocarrier in a multienzyme labeling amplification strategy for ultrasensitive electrochemical immunoassay of phosphorylated p53 (S392), Anal. Chem. 83 (2011) 746–752.
[48] L. Shen, Z. Chen, Y. Li, S. He, S. Xie, X. Xu, et al., Electrochemical DNAzyme sensor for lead based on amplification of DNA-Au bio-bar codes, Anal. Chem. 80 (2008) 6323–6328.
[49] Y. Huang, J. Chen, S. Zhao, M. Shi, Z.-F. Chen, H. Liang, Label-free colorimetric aptasensor based on nicking enzyme assisted signal amplification and DNAzyme amplification for highly sensitive detection of protein, Anal. Chem. 85 (2013) 4423–4430.
[50] X.-H. Zhao, L. Gong, X.-B. Zhang, B. Yang, T. Fu, R. Hu, et al., Versatile DNAzyme-based amplified biosensing platforms for nucleic acid, protein, and enzyme activity detection, Anal. Chem. 85 (2013) 3614–3620.
[51] M.B. Gholivand, M. Shamsipur, S. Dehdashtian, H.R. Rajabi, Development of a selective and sensitive voltammetric sensor for propylparaben based on a nanosized molecularly imprinted polymer-carbon paste electrode, Mater. Sci. Eng. C Mater. Biol. Appl. 36 (2014) 102–107.
[52] Y. Kong, X. Shan, J. Ma, M. Chen, Z. Chen, A novel voltammetric sensor for ascorbic acid based on molecularly imprinted poly(*o*-phenylenediamine-*co*-*o*-aminophenol), Anal. Chim. Acta 809 (2014) 54–60.
[53] Y. Yamamoto, Y. Ohno, K. Maehashi, K. Matsumoto, Noise reduction of carbon nanotube field-effect transistor biosensors by alternating current measurement, Jpn J. Appl. Phys. 48 (2009) 06FJ01.
[54] C. March, J.V. García, Á. Sánchez, A. Arnau, Y. Jiménez, P. García, et al., High-frequency phase shift measurement greatly enhances the sensitivity of QCM immunosensors, Biosens. Bioelectron. 65 (2015) 1–8.
[55] M. Yang, A. Javadi, S. Gong, Sensitive electrochemical immunosensor for the detection of cancer biomarker using quantum dot functionalized graphene sheets as labels, Sens. Actuators B 155 (2011) 357–360.
[56] T. Li, M. Yang, H. Li, Label-free electrochemical detection of cancer marker based on graphene-cobalt hexacyanoferrate nanocomposites, J. Electroanal. Chem. 655 (2011) 50–55.
[57] A. Zani, S. Laschi, M. Mascini, G. Marrazza, A new electrochemical multiplexed assay for PSA cancer marker detection, Electroanalysis 23 (2011) 91–99.

[58] Y. Wan, W. Deng, Y. Su, X. Zhu, C. Peng, H. Hu, et al., Carbon nanotube-based ultrasensitive multiplexing electrochemical immunosensor for cancer biomarkers, Biosens. Bioelectron. 30 (2011) 93–99.

[59] J. Tian, J. Huang, Y. Zhao, S. Zhao, Electrochemical immunosensor for prostate-specific antigen using a glassy carbon electrode modified with a nanocomposites containing gold nanoparticles supported with starch-functionalized multi-walled carbon nanotubes, Microchim. Acta 178 (2012) 81–88.

[60] Y. Li, J. Han, R. Chen, X. Ren, Q. Wei, Label electrochemical immunosensor for prostate-specific antigen based on graphene and silver hybridized mesoporous silica, Anal. Biochem. 469 (2015) 76–82.

[61] B.S. Munge, A.L. Coffey, J.M. Doucette, B.K. Somba, R. Malhotra, V. Patel, et al., Nanostructured immunosensor for attomolar detection of cancer biomarker interleukin-8 using massively labeled superparamagnetic particles, Angew. Chem. Int. Ed. Engl. 50 (2011) 7915–7918.

[62] C.K. Tang, A. Vaze, J.F. Rusling, Fabrication of immunosensor microwell arrays from gold compact discs for detection of cancer biomarker proteins, Lab Chip 12 (2012) 281–286.

[63] P.-Z. Liu, X.-W. Hu, C.-J. Mao, H.-L. Niu, J.-M. Song, B.-K. Jin, et al., Electrochemiluminescence immunosensor based on graphene oxide nanosheets/polyaniline nanowires/CdSe quantum dots nanocomposites for ultrasensitive determination of human interleukin-6, Electrochim. Acta 113 (2013) 176–180.

[64] I. Ojeda, M. Moreno-Guzmán, A. González-Cortés, P. Yáñez-Sedeño, J.M. Pingarrón, Electrochemical magnetoimmunosensor for the ultrasensitive determination of interleukin-6 in saliva and urine using poly-HRP streptavidin conjugates as labels for signal amplification, Anal. Bioanal. Chem. 406 (2014) 6363–6371.

[65] Y. Lou, T. He, F. Jiang, J.-J. Shi, J.-J. Zhu, A competitive electrochemical immunosensor for the detection of human interleukin-6 based on the electrically heated carbon electrode and silver nanoparticles functionalized labels, Talanta 122 (2014) 135–139.

[66] G. Wang, X. Hea, L. Chen, Y. Zhu, X. Zhang, Ultrasensitive IL-6 electrochemical immunosensor based on Au nanoparticles-graphene-silica biointerface, Colloids Surf. B. Biointerfaces 116 (2014) 714–719.

[67] G. Yang, L. Li, R.K. Rana, J.-J. Zhu, Assembled gold nanoparticles on nitrogen-doped graphene for ultrasensitive electrochemical detection of matrix metalloproteinase-2, Carbon 61 (2013) 357–366.

[68] E. Song, D. Cheng, Y. Song, M. Jiang, J. Yu, Y. Wang, A graphene oxide-based FRET sensor for rapid and sensitive detection of matrix metalloproteinase 2 in human serum sample, Biosens. Bioelectron. 47 (2013) 445–450.

[69] Z. Yin, Y. Wang, T.-T. Zheng, R. Zhang, X. Li, J.L. Zhu, et al., 3D label-free matrix metalloproteinase-3 immunosensor based on graphene oxide/polypyrrole-ionic liquid nanocomposites, Sci. Adv. Mater. 7 (2015) 1581–1588.

[70] N. Gan, Y. Wu, F. Hu, T. Li, L. Zheng, Y. Cao, One novel nano magnetic Fe_3O_4/ZrO_2/nano Au composite membrane modified amperometric immunosensor for α-fetoprotein in human serum, Int. J. Electrochem. Sci. 6 (2011) 461–474.

[71] Y.-J. Li, M.-J. Ma, J.-J. Zhu, Dual-signal amplification strategy for ultrasensitive photoelectrochemical immunosensing of αfetoprotein, Anal. Chem. 84 (2012) 10492–10499.

[72] S. Ge, L. Ge, M. Yan, X. Song, J. Yu, J. Huang, A disposable paper-based electrochemical sensor with an addressable electrode array for cancer screening, Chem. Commun. 48 (2012) 9397–9399.

[73] G. Lai, L. Wang, J. Wu, H. Ju, F. Yan, Electrochemical stripping analysis of nanogold label-induced silver deposition for ultrasensitive multiplexed detection of tumor markers, Anal. Chim. Acta 721 (2012) 1–6.

[74] H. Wang, X. Li, K. Mao, Y. Li, B. Du, Y. Zhang, et al., Electrochemical immunosensor for α-fetoprotein detection using ferroferric oxide and horseradish peroxidase as signal amplification labels, Anal. Biochem. 465 (2014) 121–126.

[75] X. Gao, Y. Zhang, H. Chen, Z. Chen, X. Lin, Amperometric immunosensor for carcinoembryonic antigen detection with carbon nanotube-based film decorated with gold nanoclusters, Anal. Biochem. 414 (2011) 70–76.

[76] J. Han, Y. Zhuo, Y.-Q. Chai, L. Mao, Y.-L. Yuan, R. Yuan, Highly conducting gold nanoparticles–graphene nanohybrid films for ultrasensitive detection of carcinoembryonic antigen, Talanta 85 (2011) 130–135.

[77] F.-Y. Kong, M.-T. Xu, J.-J. Xu, H.-Y. Chen, A novel label-free electrochemical immunosensor for carcinoembryonic antigen based on gold nanoparticles-thionine-reduced graphene oxide nanocomposite film modified glassy carbon electrode, Talanta 85 (2011) 2620–2625.

[78] P. Wang, L. Ge, M. Yan, X. Song, S. Ge, J. Yu, Paper-based three-dimensional electrochemical immunodevice based on multi-walled carbon nanotubes functionalized paper for sensitive point-of-care testing, Biosens. Bioelectron. 32 (2012) 238–243.

[79] R. Wang, X. Chen, J. Ma, Z. Ma, Ultrasensitive detection of carcinoembryonic antigen by a simple label-free immunosensor, Sens. Actuators B 176 (2013) 1044–1050.

[80] D. Lin, J. Wu, H. Ju, F. Yan, Nanogold/mesoporous carbon foam-mediated silver enhancement for graphene-enhanced electrochemical immunosensing of carcinoembryonic antigen, Biosens. Bioelectron. 52 (2014) 153–158.

[81] G. Sun, Y.-N. Ding, C. Ma, Y. Zhang, S. Ge, J. Yu, et al., Paper-based electrochemical immunosensor for carcinoembryonic antigen based on three dimensional flower-like gold electrode and gold-silver bimetallic nanoparticles, Electrochim. Acta 147 (2014) 650–656.

[82] V. Vermeeren, L. Grieten, N. Vanden Bon, N. Bijnens, S. Wenmackers, S.D. Janssens, et al., Impedimetric, diamond-based immunosensor for the detection of C-reactive protein, Sens. Actuators B 157 (2011) 130–138.

[83] N. Gan, L. Meng, F. Hu, Y. Cao, Y. Wu, L. Jia, et al., A renewable amperometric immunosensor for hs-CRP based on functionalized Fe_3O_4@Au magnetic nanoparticles attracted on Fe (III) phthlocyanine/chitosan-membrane modified screen-printed carbon electrode by a magnet, Appl. Mech. Mater. 110–116 (2012) 519–526.

[84] Z.H. Ibupoto, N. Jamal, K. Khun, M. Willander, Development of a disposable potentiometric antibody immobilized ZnO nanotubes based sensor for the detection of C-reactive protein, Sens. Actuators B 166–167 (2012) 809–814.

[85] B. Esteban-Fernández de Ávila, V. Escamilla-Gómez, S. Campuzano, M. Pedrero, J.M. Pingarrón, Ultrasensitive amperometric magnetoimmunosensor for human C-reactive protein quantification in serum, Anal. Chim. Acta 784 (2013) 18–24.

[86] T. Bryan, X. Luo, P.R. Bueno, J.J. Davis, An optimised electrochemical biosensor for the label-free detection of C-reactive protein in blood, Biosens. Bioelectron. 39 (2013) 94–98.

[87] J. Zhou, N. Gan, T. Li, H. Zhou, X. Li, Y. Cao, et al., Ultratrace detection of C-reactive protein by a piezoelectric immunosensor based on Fe_3O_4@SiO_2 magnetic capture nanoprobes and HRP-antibody co-immobilized nano gold as signal tags, Sens. Actuators B 178 (2013) 494–500.

[88] C.I.L. Justino, K. Duarte, S. Lucas, P. Chaves, P. Bettencourt, A.C. Freitas, et al., Assessment of cardiovascular disease risk using immunosensors for determination of C-reactive protein levels in serum and saliva: a pilot study, Bioanalysis 6 (2014) 1459–1470.

[89] B. Esteban-Fernández de Ávila, V. Escamilla-Gómez, V. Lanzone, S. Campuzano, M. Pedrero, D. Compagnone, et al., Multiplexed determination of amino-terminal pro-B type natriuretic peptide and C-reactive protein cardiac biomarkers in human serum at a disposable electrochemical magnetoimmunosensor, Electroanalysis 26 (2014) 254–261.

[90] Y. Zhuo, W. Yi, W. Lian, R. Yuan, Y. Chai, A. Chen, et al., Ultrasensitive electrochemical strategy for NT-proBNP detection with gold nanochains and horseradish peroxidase complex amplification, Biosens. Bioelectron. 26 (2011) 2188–2193.

[91] W. Yi, W. Liang, P. Li, S. Li, Z. Zhang, M. Yang, et al., Application of a Fab fragment of monoclonal antibody specific to N-terminal pro-brain natriuretic peptide for the detection based on regeneration-free electrochemical immunosensor, Biotechnol. Lett. 33 (2011) 1539–1543.

[92] B. Esteban-Fernández de Ávila, V. Escamilla-Gómez, S. Campuzano, M. Pedrero, J.M. Pingarrón, Disposable amperometric magnetoimmunosensor for the sensitive detection of the cardiac biomarker amino-terminal pro-B-type natriuretic peptide in human serum, Anal. Chim. Acta 784 (2013) 18–24.

[93] R.A.S. Fonseca, J. Ramos-Jesus, L.T. Kubot, R.F. Dutra, A nanostructured piezoelectric immunosensor for detection of human cardiac troponin T, Sensors (Basel) 11 (2011) 10785–10797.

[94] S.L.R. Gomes-Filho, A.C.M.S. Dias, M.M.S. Silva, B.V.M. Silva, R.F. Dutra, A carbon nanotube-based electrochemical immunosensor for cardiac troponin T, Microchem. J. 109 (2013) 10–15.

[95] B.V.M. Silva, I.T. Cavalcanti, M.M.S. Silva, R.F. Dutra, A carbon nanotube screen-printed electrode for label-free detection of the human cardiac troponin T, Talanta 117 (2013) 431–437.

[96] A.B. Mattos, T.A. Freitas, L.T. Kubota, R.F. Dutra, An o-aminobenzoic acid film-based immunoelectrode for detection of the cardiac troponin T in human serum, Biochem. Eng. J. 71 (2013) 97–104.

[97] A.J.S. Ahammad, Y.H. Choi, K. Koh, J.H. Kim, J.J. Lee, M. Lee, Electrochemical detection of cardiac biomarker Troponin I at gold nanoparticle-modified ITO electrode by using open circuit potential, Int. J. Electrochem. Sci. 6 (2011) 1906–1916.

[98] K.K. Jagadeesan, S. Kumar, G. Sumana, Application of conducting paper for selective detection of troponin, Electrochem. Commun. 20 (2012) 71–74.

[99] S. Singal, A.K. Srivastava, A.M. Biradar, A. Mulchandani, Rajesh, Pt nanoparticles-chemical vapor deposited graphene composite based immunosensor for the detection of human cardiac troponin I, Sens. Actuators B 205 (2014) 363–370.

[100] J.-H. Cho, M.-H. Kim, R.-S. Mok, J.-W. Jeon, G.-S. Lim, C.-Y. Chai, et al., Two-dimensional paper chromatography-based fluorescent immunosensor for detecting acute myocardial infarction markers, J. Chromatogr. B. Analyt Technol Biomed Life Sci. 967 (2014) 139–146.

[101] E.V. Suprun, A.L. Shilovskaya, A.V. Lisitsa, T.V. Bulko, V.V. Shumyantseva, A.I. Archakov, Electrochemical immunosensor based on metal nanoparticles for cardiac myoglobin detection in human blood plasma, Electroanalysis 23 (2011) 1051–1057.

[102] E. Zapp, E. Westphal, H. Gallardo, B. de Souza, I.C. Vieira, Liquid crystal and gold nanoparticles applied to electrochemical immunosensor for cardiac biomarker, Biosens. Bioelectron. 59 (2014) 127–133.

[103] D.-H. Kim, S.-M. Seo, H.-M. Cho, S.-J. Hong, D.-S. Lim, S.-H. Paek, Continuous immunosensing of myoglobin in human serum as potential companion diagnostics technique, Biosens. Bioelectron. 62 (2014) 234–241.

[104] K. Masuhara, T. Nakai, K. Yamaguchi, S. Yamasaki, Y. Sasaguri, Significant increases in serum and plasma concentrations of matrix metalloproteinases 3 and 9 in patients with rapidly destructive osteoarthritis of the hip, Arthritis Rheum. 46 (2002) 2625–2631.

[105] R. Malhotra, V. Patel, J.P. Vaqué, J.S. Gutkind, J.F. Rusling, Ultrasensitive electrochemical immunosensor for oral cancer biomarker IL-6 using carbon nanotube forest electrodes and multilabel amplification, Anal. Chem. 82 (2010) 3118–3123.

[106] K.-J. Huang, D.-J. Niu, W.-Z. Xie, W. Wang, A disposable electrochemical immunosensor for carcinoembryonic antigen based on nano-Au/multi-walled carbon nanotubes-chitosans nanocomposite film modified glassy carbon electrode, Anal. Chim. Acta 659 (2010) 102–108.
[107] J.A. Ho, Y.-C. Lin, L.-S. Wang, K.-C. Hwang, P.-T. Chou, Carbon nanoparticle-enhanced immunoelectrochemical detection for protein tumor marker with cadmium sulfide biotracers, Anal. Chem. 81 (2009) 1340–1346.
[108] X. Che, R. Yuan, Y. Chai, J. Li, Z. Song, J. Wang, Amperometric immunosensor for the determination of α-1-fetoprotein based on multiwalled carbon nanotube-silver nanoparticle composite, J. Colloid Interface Sci. 345 (2010) 174–180.
[109] V.L. Roger, A.S. Go, D.M. Lloyd-Jones, E.J. Benjamin, J.D. Berry, W.B. Borden, et al., Heart disease and stroke statistics – 2012 update. A report from the American Heart Association, Circulation 125 (2012) 2–220.
[110] C.I.L. Justino, A.C. Freitas, J.P. Amaral, T.A.P. Rocha-Santos, S. Cardoso, A.C. Duarte, Disposable immunosensors for C-reactive protein based on carbon nanotubes field effect transistors, Talanta 108 (2013) 165–170.
[111] S.K. Pasha, A. Kaushik, A. Vasudev, S.A. Snipes, S. Bhansali, Electrochemical immunosensing of saliva cortisol, J. Electrochem. Soc. 161 (2014) 3077–3082.
[112] P.K. Vabbina, A. Kaushik, N. Pokhrel, S. Bhansali, N. Pala, Electrochemical cortisol immunosensors based on sonochemically synthesized zinc oxide 1D nanorods and 2D nanoflakes, Biosens. Bioelectron. 63 (2015) 124–130.
[113] G. Hao, D. Zheng, T. Gan, C. Hu, S. Hu, Development and application of estradiol sensor based on layer-by-layer assembling technique, J. Experim. Nanosci. 6 (2011) 13–28.
[114] I. Ojeda, J. Lopez-Montero, M. Moreno-Guzman, B.C. Janegitz, A. Gonzalez-Cortes, P. Yanez-Sedeno, et al., Electrochemical immunosensor for rapid and sensitive determination of estradiol, Anal. Chim. Acta 743 (2012) 117–124.
[115] Z. Wang, P. Wang, X. Tu, Y. Wu, G. Zhan, C. Li, A novel electrochemical sensor for estradiol based on nanoporous polymeric film bearing poly{1-butyl-3-[3-(N-pyrrole)propyl]imidazole dodecyl sulfonate} moiety, Sens. Actuators B 193 (2014) 190–197.
[116] H. Nie, Z. Yao, X. Zhou, Z. Yang, S. Huang, Nonenzymatic electrochemical detection of glucose using well-distributed nickel nanoparticles on straight multi-walled carbon nanotubes, Biosens. Bioelectron. 30 (2011) 28–34.
[117] Y. Zhang, Y. Wang, J. Jia, J. Wang, Nonenzymatic glucose sensor based on graphene oxide and electrospun NiO nanofibers, Sens. Actuators B 171–172 (2012) 580–587.
[118] N.Q. Dung, D. Patil, H. Jung, D. Kim, A high-performance nonenzymatic glucose sensor made of CuO–SWCNT nanocomposites, Biosens. Bioelectron. 42 (2013) 280–286.
[119] H.-W. Yang, M.-Y. Hua, S.-L. Chen, R.-Y. Tsai, Reusable sensor based on high magnetization carboxyl-modified graphene oxide with intrinsic hydrogen peroxide catalytic activity for hydrogen peroxide and glucose detection, Biosens. Bioelectron. 41 (2013) 172–179.
[120] G.-X. Zhong, W.-X. Zhang, Y.-M. Sun, Y.-Q. Wei, Y. Lei, H.-P. Peng, et al., A nonenzymatic amperometric glucose sensor based on three dimensional nanostructure gold electrode, Sens. Actuators B 212 (2015) 72–77.
[121] J. Zhang, J. Ma, S. Zhang, W. Wang, Z. Chen, A highly sensitive nonenzymatic glucose sensor based on CuO nanoparticles decorated carbon spheres, Sens. Actuators B 211 (2015) 385–391.
[122] L. Hong, A.-L. Liu, G.-W. Li, W. Chen, X.-H. Lin, Chemiluminescent cholesterol sensor based on peroxidase-like activity of cupric oxide nanoparticles, Biosens. Bioelectron. 43 (2013) 1–5.
[123] A. Umar, R. Ahmad, S.W. Hwang, S.H. Kim, A. Al-Hajry, Y.B. Hahn, Development of highly sensitive and selective cholesterol biosensor based on cholesterol oxidase co-immobilized with α-Fe_2O_3 micro-pine shaped hierarchical structures, Electrochim. Acta 135 (2014) 396–403.
[124] R. Ahmad, N. Tripathy, S.H. Kim, A. Umar, A. Al-Hajry, Y.-B. Hahn, High performance cholesterol sensor based on ZnO nanotubes grown on Si/Ag electrodes, Electrochem. Commun. 38 (2014) 4–7.
[125] M.M. Rahman, Fabrication of a highly-sensitive acetylcholine sensor based on AChOx immobilized smart-chips, Sens. Transducers J. 126 (2011) 11–18.
[126] L. Zhang, J. Chen, Y. Wang, L. Yu, J. Wang, H. Peng, et al., Improved enzyme immobilization for enhanced bioelectrocatalytic activity of choline sensor and acetylcholine sensor, Sens. Actuators B 193 (2014) 904–910.
[127] S. Pundir, N. Chauhan, J. Narang, C.S. Pundir, Amperometric choline biosensor based on multiwalled carbon nanotubes/zirconium oxide nanoparticles electrodeposited on glassy carbon electrode, Anal. Biochem. 427 (2012) 26–32.
[128] E. Akyilmaz, M. Turemis, I. Yasa, Voltammetric determination of epinephrine by white rot fungi (*Phanerochaete chrysosporium* ME446) cells based microbial biosensor, Biosens. Bioelectron. 26 (2011) 2590–2594.
[129] L.I.B. Silva, A.M. Gomes, M.M. Pintado, H. Pinheiro, D. Moura, A.C. Freitas, et al., Optical fiber bioanalyzer based on enzymatic coating matrix for catecholamines and their metabolites assessment in patients with Down syndrome, IEEE Sens. J. 12 (2012) 76–84.
[130] L. Silva, K. Duarte, A.C. Freitas, T.S.L. Panteleitchouk, T.A.P. Rocha-Santos, M.E. Pereira, et al., Fluorescence-based optical fiber analyzer for catecholamines determination, Anal. Methods 4 (2012) 2300–2306.
[131] W.S. Gozansky, J.S. Lynn, M.L. Laudenslager, W.M. Kohrt, Salivary cortisol determined by enzyme immunoassay is preferable to serum total cortisol for assessment of dynamic hypothalamic-pituitary-adrenal axis activity, Clin. Endocrinol. (Oxf) 63 (2005) 336–341.
[132] P.C. Nien, T.S. Tung, K.C. Ho, Amperometric glucose biosensor based on entrapment of glucose oxidase in a poly(3,4-ethylenedioxythiophene) Film, Electroanalysis 18 (2006) 1408–1415.
[133] E. Salinas, V. Rivero, A.A.J. Torriero, D. Benuzzi, M.I. Sanz, J. Raba, Multienzymatic-rotating biosensor for total cholesterol determination in a FIA System, Talanta 70 (2006) 244–250.
[134] S. Lin, C.C. Liu, T.C. Chou, Amperometric acetylcholine sensor catalyzed by nickel anode electrode, Biosens. Bioelectron. 20 (2004) 9–14.
[135] R.T. Peaston, C. Weinkove, Measurement of catecholamines and their metabolites, Ann. Clin. Biochem. 41 (2004) 17–38.
[136] S.K. Arya, G. Chornokur, M. Venugopal, S. Bhansali, Dithiobis(succinimidyl propionate) modified gold microarray electrode based electrochemical immunosensor for ultrasensitive detection of cortisol, Biosens. Bioelectron. 25 (2010) 2296–2301.
[137] Y. Yang, S. Kim, J. Chae, Separating and detecting *Escherichia coli* in a microfluidic channel for urinary tract infection applications, J. Microelectromech. Syst. 20 (2011) 819–826.
[138] M. Safavieh, M.U. Ahmed, M. Tolba, M. Zourob, Microfluidic electrochemical assay for rapid detection and quantification of *Escherichia coli*, Biosens. Bioelectron. 31 (2012) 523–528.
[139] M. Barreiros dos Santos, S. Azevedo, J.P. Agusil, B. Prieto-Simón, C. Sporer, E. Torrents, et al., Label-free ITO-based immunosensor for the detection of very low concentrations of pathogenic bacteria, Bioelectrochemistry 101 (2015) 146–152.
[140] A. Ahmed, J.V. Rushworth, J.D. Wright, P.A. Millner, Novel impedimetric immunosensor for detection of pathogenic bacteria *Streptococcus pyogenes* in human saliva, Anal. Chem. 85 (2013) 12118–12125.
[141] C. Ma, G. Xie, W. Zhang, M. Liang, B. Liu, H. Xiang, Label-free sandwich type of immunosensor for hepatitis C virus core antigen based on the use of gold nanoparticles on a nanostructured metal oxide surface, Mikrochim. Acta 178 (2012) 331–340.
[142] C. Ma, M. Liang, L. Wang, H. Xiang, Y. Jiang, Y. Li, et al., MultisHRP-DNA-coated CMWNTs as signal labels for an ultrasensitive hepatitis C virus core antigen electrochemical immunosensor, Biosens. Bioelectron. 47 (2013) 467–474.
[143] R. Singh, A. Sharma, S. Hong, J. Jang, Electrical immunosensor based on dielectrophoretically-deposited carbon nanotubes for detection of influenza virus H1N1, Analyst 139 (2014) 5415–5421.
[144] C.-H. Zhou, Y.-M. Long, B.-P. Qi, D.-W. Pang, Z.-L. Zhang, A magnetic bead-based bienzymatic electrochemical immunosensor for determination of H9N2 avian influenza virus, Electrochem. Commun. 31 (2013) 129–132.
[145] A.C.M.S. Dias, S.L.R. Gomes-Filho, M.M.S. Silva, R.F. Dutra, A sensor tip based on carbon nanotube-ink printed electrode for the dengue virus NS1 protein, Biosens. Bioelectron. 44 (2013) 216–221.
[146] T. Zheng, J.-J. Fu, L. Hu, F. Qiu, M. Hu, J.-J. Zhu, et al., Nanoarchitectured electrochemical cytosensors for selective detection of leukemia cells and quantitative evaluation of death receptor expression on cell surfaces, Anal. Chem. 85 (2013) 5609–5616.
[147] J. Liu, Y. Qin, D. Li, T. Wang, Y. Liu, J. Wang, et al., Highly sensitive and selective detection of cancer cell with a label-free electrochemical cytosensor, Biosens. Bioelectron. 41 (2013) 436–441.
[148] T.A. Mir, J.-H. Yoon, N.G. Gurudatt, M.-S. Won, Y.-B. Shim, Ultrasensitive cytosensing based on an aptamer modified nanobiosensor with a bioconjugate: detection of human non-small-cell lung cancer cells, Biosens. Bioelectron. 74 (2015) 594–600.
[149] D. Sun, J. Lu, Z. Chen, Y. Yu, M. Mo, A repeatable assembling and disassembling electrochemical aptamer cytosensor for ultrasensitive and highly selective detection of human liver cancer cells, Anal. Chim. Acta 885 (2015) 166–173.
[150] D. Sun, J. Lu, Y. Zhong, Y. Yu, Y. Wang, B. Zhang, et al., Sensitive electrochemical aptamer cytosensor for highly specific detection of cancer cells based on the hybrid nanoelectrocatalysts and enzyme for signal amplification, Biosens. Bioelectron. 75 (2016) 301–307.
[151] M. Barreiros dos Santos, J.P. Agusil, B. Prieto-Simon, C. Sporer, V. Teixeira, J. Samitier, Highly sensitive detection of pathogen *Escherichia coli* O157:H7 by electrochemical impedance spectroscopy, Biosens. Bioelectron. 45 (2013) 174–180.
[152] X. Fang, O.K. Tan, M.S. Tse, E.E. Ooi, A label-free immunosensor for diagnosis of dengue infection with simple electrical measurements, Biosens. Bioelectron. 25 (2010) 1137–1142.
[153] S. Kumbhat, K. Sharma, R. Gehlot, A. Solanki, V. Joshi, Surface plasmon resonance based immunosensor for serological diagnosis of dengue virus infection, J. Pharm. Biomed. Anal. 52 (2010) 255–259.
[154] T. Pfaffe, J. Cooper-White, P. Beyerlein, K. Kostner, C. Punyadeera, Diagnostic potential of saliva: current state and future applications, Clin. Chem. 57 (2011) 675–687.
[155] Clinical and Laboratory Standards Institute (CLSI), Interference Testing in Clinical Chemistry; Approved Guideline, second ed., CLSI Document EP7-A2, Clinical and Laboratory Standards Institute, USA, 2005. ISBN 1-56238-584-4.